

Qutrit and Ququint Magic States

Akalank Jain and Shiroman Prakash

*Department of Physics and Computer Science, Dayalbagh Educational Institute, Dayalbagh,
Agra, India 282005*

Abstract

Non-stabilizer eigenstates of Clifford operators are natural candidates for endpoints of magic state distillation routines. We provide an explicit bestiary of all inequivalent non-stabilizer Clifford eigenstates for qutrits and ququints. For qutrits, there are four non-degenerate eigenstates, and two families of degenerate eigenstates. For ququints, there are eight non-degenerate eigenstates, and three families of degenerate eigenstates. Of these states, a simultaneous eigenvector of all Clifford symplectic rotations known as the qutrit *strange state* is distinguished as both the most magic qutrit state and the most symmetric qutrit state. We show that no analogue of the qutrit strange state (i.e., no simultaneous eigenvector of all symplectic rotations) exists for qudits of any odd prime dimension $d > 3$.

Contents

1	Introduction	2
2	Preliminaries	3
2.1	The Qudit Pauli Group and Clifford Group	3
2.2	Discrete Wigner Functions	4
2.3	Measures of Magic	5
3	Eigenstates of Qutrit Clifford Operators	6
3.1	Conjugacy Classes of the Single Qutrit Clifford Group	7
3.2	Qutrit Clifford Eigenstates	10
3.2.1	The Strange State $ S\rangle$	11
3.2.2	The State $ H_+\rangle$	13
3.2.3	The Norell State $ N_+\rangle$	14
3.2.4	The State $ XV_{\hat{S}}\rangle$	14
3.2.5	Degenerate Eigenstates of V_{-1}	15
3.2.6	Degenerate Eigenstates of $V_{\hat{S}}$	15
4	Eigenstates of Ququint Clifford Operators	16
4.1	Conjugacy Classes of the Single-Ququint Clifford group	16
4.2	Ququint Clifford Eigenstates	18
5	Twirling Schemes	20
5.1	Qutrits	23
5.1.1	Twirling Schemes for H States	23
5.1.2	Twirling Schemes for N States	24
5.1.3	Twirling Schemes for $XV_{\hat{S}}$ States	25
5.1.4	Twirling Schemes for Degenerate Families of States	25
5.2	Ququints	25
5.2.1	Twirling Scheme for the State $ H, -1\rangle$	25
5.2.2	Twirling Scheme for the State $ B', -1\rangle$	27
6	Uniqueness of the Qutrit Strange State	27

1 Introduction

Magic state distillation [1, 2] is an approach to fault tolerant quantum computing that relies on ancilla qudits in non-stabilizer states to promote the Clifford group to universal quantum computation. [3] Magic state distillation for qubits is a rich and well-studied subject (e.g., [1, 2, 4–12]). Magic state distillation for qudits of other dimensions is less well-studied, but has attracted some interest [13–16] in the past few years.

While there appear to be practical advantages to using qudits instead of qubits [15, 17], there are also theoretical motivations to study qudit magic state distillation. In particular, qudit magic state distillation has been used to identify contextuality as a resource for universal quantum computation [18, 19] and the existence of discrete Wigner functions offers new possibilities for defining a resource theory of non-stabilizer states [20–24] not available for qubits. Given these motivations, we feel it is worthwhile to explore the state space of qudits of the smallest odd-prime dimensions, i.e., qutrits and ququints. We also remark that a variety of experimental realizations of qutrits do exist (e.g., [25–27].)

Both qubit magic states identified in [1], $|H\rangle$ and $|T\rangle$ are eigenstates of Clifford operators. Their symmetry properties under Clifford transformations can easily be visualized using the stabilizer octahedron inscribed within Bloch sphere. For example, $|H\rangle$ states directly lying above edges of the stabilizer octahedron, and hence there are 12 in total. $|T\rangle$ states lie directly above faces of the stabilizer octahedron, and hence there are 6 in total. $|T\rangle$ states are farther from the stabilizer octahedron than $|H\rangle$ states, so they may, in principle, be distilled with higher threshold to noise. In contrast, qudit state space is substantially more abstract (see, e.g., [28–34]). To overcome this difficulty, we perform some elementary but hopefully useful calculations with a view towards facilitating future work on qudit magic state distillation.

In particular, to identify states that may be candidates for endpoints of magic state distillation routines, we explicitly enumerate the eigenstates of single-qutrit and single-ququint Clifford operators, and study their symmetries under Clifford transformations.¹ We consider candidate magic states to be equivalent if they related to each other by a Clifford unitary.

For qutrits, we find that there are five inequivalent non-degenerate Clifford eigenstates, and two inequivalent one-complex-parameter families of degenerate qutrit Clifford eigenstates. For ququints, we find that there are nine inequivalent non-degenerate Clifford eigenstates, three inequivalent one-complex-parameter families of degenerate Clifford eigenstates. and one two-complex-parameter family of degenerate Clifford eigenstates. For qutrits, most of these states have been previously identified in the literature [23, 20, 13, 14, 16] in the context of qutrit magic state distillation; though an one of the degenerate families of states has not been previously discussed in the literature. For ququints, most of these states appear unstudied, but some discussion of the equatorial magic state (the state $|C\rangle$ defined below)

¹It is not necessary in principle, for magic states to be eigenstates of Clifford operators. For example, the qubit state $|\pi/3\rangle = \frac{1}{\sqrt{2}}(|0\rangle + e^{i\pi/3}|1\rangle)$ is the endpoint of a distillation routine [16], and can be used for state injection, though it is not an eigenstate of a Clifford operator. However it appears easier to construct distillation schemes for Clifford eigenstates.

appears in [15, 35, 36], and also [20]. These states are depicted in Figure 1 and Figure 4, which illustrates their symmetry properties under Clifford transformations.

The *mana* of a state, introduced in [23], is a calculable measure of its usefulness as a magic state. We calculate the mana of each of the above states, and use these results to determine the most magic qutrit and ququint eigenstate; for qutrits, it is necessary to use an related quantity, known as thauma [24, 37], as a tie-breaker. The most magic qutrit state is the strange state, $|S\rangle$, which was identified in [23], and the most magic ququint state is $|B, -e^{2\pi i/3}\rangle$, defined in section 4. We also numerically verify that these states maximize mana over all pure qutrit and ququint states.

The size of the orbit of each state under the Clifford group is a measure of how “symmetric” a state is, under Clifford transformations, with smaller orbits corresponding to more symmetric states. We compute this quantity for each of the non-degenerate eigenstates, and find that the strange state is the most symmetric qutrit Clifford eigenstate, while the state $|B, -1\rangle$ defined in section 4 is the most symmetric ququint Clifford eigenstate.

In section 5, we show how to use these results to construct twirling schemes that can be used prior magic state distillation for each of the candidate magic states. Magic state distillation routines for states $|N_+\rangle$, $|H_+\rangle$, and $|XV_{\hat{S}}\rangle$, as well as some states of the form $|2, \alpha, \beta\rangle$ have been presented in [13, 14, 16]. Distillation routines with the state $|S\rangle$ were not known until recently.

The qutrit strange state is distinguished as not only the most magic state but also the most symmetric qutrit Clifford eigenstate. The size of its orbit under the Clifford group is 9, because it is a simultaneous eigenvector of the set of symplectic rotations. In section 6, we show that the existence of such a state is unique to $d = 3$ – there is no simultaneous eigenvector of symplectic rotations for any higher odd prime. The qutrit strange state, is therefore, particularly special amongst all qudit Clifford eigenstates.

Related work, in the context of SIC-POVMs, appears in [38–42, 32]. Alternative approaches to magic states as eigenstates of permutation operators appear in [43–45].

2 Preliminaries

2.1 The Qudit Pauli Group and Clifford Group

The study of fault-tolerant quantum computing using qudits of odd-prime dimension is facilitated by their elegant mathematical structure, which we review here. Henceforth, we will use the word qudit to refer to a quantum system of odd prime dimension p . Let $\omega_p = e^{2\pi i/p}$ and $i, j, k, n \in \mathbb{Z}_p$.

The higher-dimensional generalization of the Pauli group, \mathcal{P}_p , also known as the Heisenberg-Weyl displacement group, and is generated by the operators

$$X |n\rangle = |n+1\rangle, \quad Z |n\rangle = \omega_p^n |n\rangle, \quad (2.1)$$

which satisfy $ZX = \omega_p XZ$. The Heisenberg-Weyl displacement operators are defined in terms of X and Z as

$$\hat{D}_{(u,v)} = \omega^{uv2^{-1}} Z^u X^v. \quad (2.2)$$

Eigenstates of Heisenberg-Weyl operators are known as stabilizer states. There are $p(p+1)$ single-qudit stabilizer states.

The Clifford group is defined as the set of all operators that map qudit Pauli operators to qudit Pauli operators:

$$\mathcal{C} = \{C \in PSU(p) | C\mathcal{P}_p C^\dagger = \mathcal{P}_p\}. \quad (2.3)$$

We consider two elements of the Clifford group to be equivalent if they differ by an overall phase (i.e., the Clifford group should be thought of as a subgroup of $PSU(p)$.)

As shown in [38], the single-qudit Clifford group (up to global phases) is isomorphic to the semi-direct product $\mathbb{Z}_p^2 \rtimes SL(2, \mathbb{Z}_p)$. Let $\hat{F} \in SL(2, \mathbb{Z}_p)$ and $u, v \in \mathbb{Z}_p$. The map from $\mathbb{Z}_p^2 \rtimes SL(2, \mathbb{Z}_p)$ states that any single-qudit Clifford operator can be written in the form $D_{(u,v)} V_{\hat{F}}$, such that the following multiplication law is obeyed,

$$D_{(u_1, v_1)} V_{\hat{F}_1} D_{(u_2, v_2)} V_{\hat{F}_2} = D_{(u_1, v_1) + F_1(u_2, v_2)} V_{\hat{F}_1 \hat{F}_2}. \quad (2.4)$$

Let $\hat{F} = \begin{pmatrix} a & b \\ c & d \end{pmatrix}$, the map $V_{\hat{F}}$ is given by:

$$V_{\hat{F}} = \begin{cases} \frac{1}{\sqrt{p}} \sum_{j,k=0}^{p-1} \omega^{2^{-1}b^{-1}(ak^2-2jk+dj^2)} |j\rangle \langle k| & b \neq 0 \\ \sum_{k=0}^{p-1} \omega^{2^{-1}ack^2} |ak\rangle \langle k| & b = 0 \end{cases}. \quad (2.5)$$

$SL(2, \mathbb{Z}_p)$ can be generated by,

$$\hat{H} = \begin{pmatrix} 0 & 1 \\ -1 & 0 \end{pmatrix}, \text{ and } \hat{S} = \begin{pmatrix} 1 & 0 \\ 0 & -1 \end{pmatrix}. \quad (2.6)$$

We refer to the set of Clifford operators of the form $V_{\hat{F}}$ as the set of *symplectic rotations*.

The single-qudit Clifford group is generated by the operators $H = V_{\hat{H}}$ and $S = Z^{2^{-1}} V_{\hat{S}}$, given by:

$$H |k\rangle = \frac{1}{\sqrt{p}} \sum_j \omega_p^{jk} |j\rangle, \quad V_{\hat{S}} |k\rangle = \omega_p^{2^{-1}k^2} |k\rangle. \quad (2.7)$$

2.2 Discrete Wigner Functions

Wigner first observed that quantum states can be represented as quasi-probability distributions over phase space. Here, we use an analog of Wigner's construction for finite-dimensional

quantum systems of prime dimension [46, 47], for which phase space is $Z_p \otimes Z_p$. In particular, the following construction of a discrete Wigner function [39, 48, 49] is particularly useful, and has been employed in [21, 18].

We define phase point operators as:

$$A_{(0,0)} = \frac{1}{p} \sum_{u=0}^{p-1} \sum_{v=0}^{p-1} \hat{D}_{(u,v)} \quad (2.8)$$

$$A_{(u,v)} = D_{(u,v)} A_{(0,0)} D_{(u,v)}^\dagger. \quad (2.9)$$

The discrete Wigner function for a state $\hat{\rho}$ is defined in terms of the phase point operators as:

$$W_{(u,v)} = \frac{1}{p} \text{tr}(\hat{\rho} A_{(u,v)}). \quad (2.10)$$

When the Wigner function is non-negative, it can be interpreted as a probability distribution on phase space. Clifford operators act as translations and symplectic rotations on the phase point operators; hence, they can be efficiently simulated acting on states with non-negative discrete Wigner function, as explained in [21].

The set of states with non-negative discrete Wigner function is a convex set known as the Wigner polytope. Perhaps surprisingly, as observed in [21], the Wigner polytope contains the stabilizer polytope, which is the set of mixtures of stabilizer states, as a proper subset. Because Clifford operations on states within the Wigner polytope can be efficiently simulated, the ability to prepare ancillas outside of the Wigner polytope is a necessary condition for magic state distillation. In [18], it was also shown that negativity of the Wigner function is equivalent to contextuality with respect to stabilizer measurements. It was also recently shown that no finite magic state distillation routine can distill states tight to the boundary of any facet of the Wigner polytope [50], generalizing a well-known result for qubits [51, 52]. (See also [53, 19, 49, 54] for related work.)

2.3 Measures of Magic

In the magic state model of quantum computation, ancilla qudits in non-stabilizer states serve as a resource for achieving universal quantum computation. This idea is made precise in [23], who formulate a resource theory for non-stabilizer states, that is inspired by the analogous resource theory of entanglement.

In [23] a (pure) *magic state* is defined to be any pure quantum state that is not a stabilizer state. The amount of magic a state possesses can be quantified via the *regularized entropy of magic*, which is defined, for a state $|\psi\rangle$ to be the minimum relative entropy between $|\psi\rangle^{\otimes n}$ and any n -qudit stabilizer state for large n . The regularized entropy of magic has several attractive properties that justify treating it as a resource, as explained in [23].

Unfortunately, the regularized entropy of magic is not possible to compute. Thanks to the existence of the discrete Wigner function in odd dimensions, two powerful computable

alternatives to regularized entropy of magic exist, the *mana* [23] and the *thauma* [24]. The reason that these measures are meaningful is that they allow us to prove rigorous bounds on the inter-convertibility between magic states using Clifford unitaries and stabilizer measurements. Suppose two quantum states ρ_1 and ρ_2 have mana (or thauma) M_1 and M_2 respectively, with $M_2 > M_1$. Any stabilizer operation that converts ρ_1 states to ρ_2 states, has a bounded rate of conversion: Suppose the process takes m ρ_1 states as input and outputs n ρ_2 states, then $\frac{m}{n} > \frac{M_2}{M_1}$.

The mana, $\mathcal{M}(\rho)$ of a state ρ is defined in terms of the sum of negative entries, $\text{sn}(\rho)$ in the discrete Wigner function of ρ , as:

$$\mathcal{M}(\rho) = \log(2\text{sn}(\rho) + 1) \quad (2.11)$$

This is a natural notion of a resource since negative entries in the discrete Wigner function act as an obstacle to classical simulation. Since the discrete Wigner function is normalized to one, it can also be written in the simpler form,

$$\mathcal{M}(\rho) = \log \left(\sum_{p,q} |W_\rho(p,q)| \right). \quad (2.12)$$

It was shown in [23] that mana is the only meaningful resource that can be defined from negativity of the Wigner function. In particular, the most-negative entry of the discrete Wigner function of a magic state is not a meaningful resource, although it does determine the best theoretical threshold of a magic state distillation scheme that distills the given state [20].

The thauma is defined in [24, 37]. We do not discuss it much here, but we note that it can provide more stringent bounds than mana.

We define the magic state that maximizes the mana as the *most magic state*. When two or more Clifford-inequivalent magic states have the same mana, we can use thauma as a tie-breaker, but this is necessary only in $d = 3$, not in $d = 5$.

We remark that it would be interesting to combine the above measures of magic, with the graph theoretic formalism of [55, 56]. Our discussion focused on qudits of odd prime dimension, some related work for qubits appears in [57, 58].

3 Eigenstates of Qutrit Clifford Operators

In this section we provide a complete enumeration of the eigenstates of Clifford operators, which are natural candidates for qutrit magic states. We consider two candidate magic states to be equivalent if they are related by a Clifford operation, i.e, $|m_1\rangle \sim |m_2\rangle$ if $|m_1\rangle = C|m_2\rangle$ for $C \in \mathcal{C}$.

Suppose two Clifford operators C_1 and C_2 are in the same conjugacy class $[C_1]$ of the Clifford group; then it is easy to see that the eigenvectors of C_1 are related to the eigenvectors

of C_2 by a Clifford transformation. Hence, we only need to consider eigenvectors of one representative of each conjugacy class of the Clifford group. It is convenient to consider two different conjugacy classes to be equivalent if they have identical eigenspaces, modulo Clifford transformations. The set of conjugacy classes modulo this equivalence relation forms the set of *reduced conjugacy classes*, denoted as $[[C]]$. (For example $[XV_{\hat{S}}]$ and $[(XV_{\hat{S}})^{-1}]$, below, are equivalent, and belong to the same reduced conjugacy class $[[XV_{\hat{S}}]]$.)

In a slight abuse of terminology we will use the phrase “eigenvectors of a conjugacy class” to mean the eigenvectors of any representative operator of that reduced conjugacy class.

3.1 Conjugacy Classes of the Single Qutrit Clifford Group

Conjugacy Classes of $SL(2, \mathbb{Z}_3)$

Let us first consider the group of symplectic rotations $SL(2, \mathbb{Z}_3)$ which is generated by \hat{H} and \hat{S} described above. The conjugacy classes of $SL(2, \mathbb{Z}_3)$ are well-known, see e.g., [39, 59], and can also be computed directly. They are

$$[\hat{1}] = \left\{ \begin{pmatrix} 1 & 0 \\ 0 & 1 \end{pmatrix} \right\} \quad (3.1)$$

$$[\hat{2}] = \left\{ \begin{pmatrix} 2 & 0 \\ 0 & 2 \end{pmatrix} \right\} \quad (3.2)$$

$$[\hat{H}] = \left\{ \begin{pmatrix} 0 & 1 \\ 2 & 0 \end{pmatrix}, \begin{pmatrix} 0 & 2 \\ 1 & 0 \end{pmatrix}, \begin{pmatrix} 1 & 1 \\ 1 & 2 \end{pmatrix}, \begin{pmatrix} 1 & 2 \\ 2 & 2 \end{pmatrix}, \begin{pmatrix} 2 & 1 \\ 1 & 1 \end{pmatrix}, \begin{pmatrix} 2 & 2 \\ 2 & 1 \end{pmatrix} \right\} \quad (3.3)$$

$$[\hat{S}] = \left\{ \begin{pmatrix} 1 & 0 \\ 1 & 1 \end{pmatrix}, \begin{pmatrix} 1 & 2 \\ 0 & 1 \end{pmatrix}, \begin{pmatrix} 2 & 2 \\ 1 & 0 \end{pmatrix}, \begin{pmatrix} 0 & 2 \\ 1 & 2 \end{pmatrix} \right\} \quad (3.4)$$

$$[\hat{S}^2] = \left\{ \begin{pmatrix} 1 & 0 \\ 2 & 1 \end{pmatrix}, \begin{pmatrix} 1 & 1 \\ 0 & 1 \end{pmatrix}, \begin{pmatrix} 2 & 1 \\ 2 & 0 \end{pmatrix}, \begin{pmatrix} 0 & 1 \\ 2 & 2 \end{pmatrix} \right\} \quad (3.5)$$

$$[\hat{N}] = \left\{ \begin{pmatrix} 2 & 0 \\ 2 & 2 \end{pmatrix}, \begin{pmatrix} 2 & 1 \\ 0 & 2 \end{pmatrix}, \begin{pmatrix} 1 & 1 \\ 2 & 0 \end{pmatrix}, \begin{pmatrix} 0 & 1 \\ 2 & 1 \end{pmatrix} \right\} \quad (3.6)$$

$$[\hat{N}^{-1}] = \left\{ \begin{pmatrix} 2 & 0 \\ 1 & 2 \end{pmatrix}, \begin{pmatrix} 2 & 2 \\ 0 & 2 \end{pmatrix}, \begin{pmatrix} 1 & 2 \\ 1 & 0 \end{pmatrix}, \begin{pmatrix} 0 & 2 \\ 1 & 1 \end{pmatrix} \right\} \quad (3.7)$$

We have defined $\hat{N} = \hat{S}\hat{H}^2$.

Let us also list the subgroups of $SL(2, \mathbb{Z}_3)$ for future use. There are 14 proper subgroups of $SL(2, \mathbb{Z}_3)$, which can be divided into 6 conjugacy classes. Apart the identity, these are:

1. One subgroup of size 8 isomorphic to the quaternion group, generated by \hat{H} and $\hat{H}' = \begin{pmatrix} 2 & 2 \\ 2 & 1 \end{pmatrix}$.

2. Four subgroups of size 6 isomorphic to \mathbb{Z}_6 , each generated by one of the elements of $[\hat{N}]$.
3. Three subgroups of size 4 isomorphic to \mathbb{Z}_4 , which are $\langle H \rangle$, $\langle H' \rangle$, or $\langle H'' = HH' \rangle$.
4. Four subgroups of size 3 isomorphic to \mathbb{Z}_3 , each generated by one of the elements of $[\hat{S}]$.
5. One subgroup of size 2 isomorphic to \mathbb{Z}_2 , generated by $\hat{2}$.

Conjugacy Classes of $\mathbb{Z}_3^2 \rtimes SL(2, \mathbb{Z}_3)$

We now turn our attention to conjugacy classes of the single qutrit Clifford group, i.e., $\mathbb{Z}_3^2 \rtimes SL(2, \mathbb{Z}_3)$. Four of the conjugacy classes of $SL(2, \mathbb{Z}_3)$ directly translate into the following conjugacy classes of the Clifford group:

$$[H] = D_{\vec{\chi}} V_{[\hat{H}]} \quad (3.8)$$

$$[N] = D_{\vec{\chi}} V_{[\hat{N}]} \quad (3.9)$$

$$[N^{-1}] = D_{\vec{\chi}} V_{[\hat{N}^{-1}]} \quad (3.10)$$

$$[V_{-1}] = D_{\vec{\chi}} V_{[\hat{2}]} \quad (3.11)$$

where $\vec{\chi}$ is any element of $\mathbb{Z}_3 \otimes \mathbb{Z}_3$.

The conjugacy class of the identity in $SL(2, \mathbb{Z}_3)$ splits into two different conjugacy classes in $\mathbb{Z}_3^2 \rtimes SL(2, \mathbb{Z}_3)$:

$$[1] = \mathbf{1} \quad (3.12)$$

$$[\text{Pauli}] = D_{\vec{\chi}} \quad (\text{for } \chi \neq \vec{0}). \quad (3.13)$$

The conjugacy classes $[S]$ and $[S^2]$, both of which contain an element of the form $\begin{pmatrix} 1 & 0 \\ \gamma & 1 \end{pmatrix}$, also split into two different conjugacy classes:

$$[V_{S^2}] = \left\{ D_{(0,v)} V_{\begin{pmatrix} 1 & 0 \\ 2 & 1 \end{pmatrix}}, D_{(u,0)} V_{\begin{pmatrix} 1 & 1 \\ 0 & 1 \end{pmatrix}}, D_{(u,-u)} V_{\begin{pmatrix} 2 & 1 \\ 2 & 0 \end{pmatrix}}, D_{(u,u)} V_{\begin{pmatrix} 0 & 1 \\ 2 & 2 \end{pmatrix}} \right\} \quad (3.14)$$

$$[XV_{S^2}] = \left\{ D_{(u^*,v)} V_{\begin{pmatrix} 1 & 0 \\ 2 & 1 \end{pmatrix}}, D_{(u,v^*)} V_{\begin{pmatrix} 1 & 1 \\ 0 & 1 \end{pmatrix}}, D_{(u,-u+v^*)} V_{\begin{pmatrix} 2 & 1 \\ 2 & 0 \end{pmatrix}}, D_{(u,u+v^*)} V_{\begin{pmatrix} 0 & 1 \\ 2 & 2 \end{pmatrix}} \right\} \quad (3.15)$$

$$[V_{\hat{S}}] = \left\{ D_{(0,v)} V_{\begin{pmatrix} 1 & 0 \\ 1 & 1 \end{pmatrix}}, D_{(u,0)} V_{\begin{pmatrix} 1 & 2 \\ 0 & 1 \end{pmatrix}}, D_{(u,-u)} V_{\begin{pmatrix} 0 & 2 \\ 1 & 2 \end{pmatrix}}, D_{(u,u)} V_{\begin{pmatrix} 2 & 2 \\ 1 & 0 \end{pmatrix}} \right\} \quad (3.16)$$

$$[XV_{\hat{S}}] = \left\{ D_{(u^*,v)} V_{\begin{pmatrix} 1 & 0 \\ 1 & 1 \end{pmatrix}}, D_{(u,v^*)} V_{\begin{pmatrix} 1 & 2 \\ 0 & 1 \end{pmatrix}}, D_{(u,-u+v^*)} V_{\begin{pmatrix} 0 & 2 \\ 1 & 2 \end{pmatrix}}, D_{(u,u+v^*)} V_{\begin{pmatrix} 2 & 2 \\ 1 & 0 \end{pmatrix}} \right\} \quad (3.17)$$

where u and v are any element of \mathbb{Z}_3 , and u^* and v^* are non-zero elements of \mathbb{Z}_3 .

In summary, there are a total of 10 conjugacy classes for the single-qutrit Clifford group. These can be grouped into the following 7 reduced conjugacy classes: $[[1]]$, $[[Z]]$, $[[V_{-1}]]$, $[[V_{\hat{S}}]]$, $[[H]]$, $[[N]]$, and $[[XV_{\hat{S}}]]$.

Eigenvectors of Clifford Conjugacy Classes

In what follows, we denote the eigenvector of an operator A with eigenvalue a as $|A, a\rangle$. If the eigenspace of A is degenerate, we write the state as $|A, a; x, y, \dots\rangle$, where x, y, \dots parameterize the degenerate eigenspace.

The reduced conjugacy class $[1]$ is trivial, and the eigenvectors of $[\text{Pauli}] = [Z]$ are stabilizer states, which are Clifford equivalent to $|0\rangle$.

Eigenvectors of $[[V_{-1}]]$

The eigenvectors of V_{-1} are

$$|V_{-1}, 1; a, b\rangle = a|0\rangle + b(|1\rangle + |2\rangle), \quad (3.18)$$

and

$$|V_{-1}, -1\rangle = (|1\rangle - |2\rangle)/\sqrt{2}. \quad (3.19)$$

Note that $V_{-1} = H^2$ coincides with the phase point operator $A_{0,0}$, [20] and commutes with H , N , and N^{-1} , so their eigenvectors are special cases of the above family of states.

Eigenvectors of $[[V_{\hat{S}}]]$

The reduced conjugacy class $[[V_{\hat{S}}]]$ includes $[V_{\hat{S}}]$ and $[V_{\hat{S}}^{-1}]$.

The eigenvectors of $V_{\hat{S}}$ are $|V_{\hat{S}}, 1\rangle = |0\rangle$ and

$$|V_{\hat{S}}, \omega^2; \gamma, \delta\rangle = \gamma|1\rangle + \delta|2\rangle. \quad (3.20)$$

Eigenvectors of $[[N]]$

$[[N]]$ includes $[N^{-1}]$ and $[N]$. The eigenvectors of N are:

$$|N, 1\rangle = |N^{-1}, 1\rangle = |0\rangle \quad (3.21)$$

$$|N, \omega^2\rangle = |N^{-1}, \omega\rangle = \frac{1}{\sqrt{2}}(|1\rangle + |2\rangle) \equiv |N_+\rangle \quad (3.22)$$

$$|N, -\omega^2\rangle = |N^{-1}, -\omega\rangle = \frac{1}{\sqrt{2}}(|1\rangle - |2\rangle). \quad (3.23)$$

The states $|N, -e^{i\pi/3}\rangle$ and $|N, e^{i\pi/3}\rangle$ are not related to each other by any Clifford operator; both are also eigenvectors of V_{-1} .

The set of convex mixtures of these states forms a planar slice of qutrit phase space. This is shown in Figure 7a.

Eigenvectors of $[[H]]$

The eigenvectors of H are:

$$|H, i\rangle = \frac{1}{\sqrt{2}} (|1\rangle - |2\rangle) \equiv |S\rangle \quad (3.24)$$

$$|H, 1\rangle = \cos \theta |0\rangle + \frac{1}{\sqrt{2}} \sin \theta (|1\rangle + |2\rangle) \equiv |H_+\rangle \quad (3.25)$$

$$|H, -1\rangle = \sin \theta |0\rangle - \frac{1}{\sqrt{2}} \cos \theta (|1\rangle + |2\rangle) \equiv |H_-\rangle, \quad (3.26)$$

where $\theta = \frac{1}{2} \arctan \sqrt{2}$.

The eigenvectors $|H, 1\rangle$ and $|H, -1\rangle$ are related to each other by the Clifford transformation $|H_1\rangle = V_{\begin{pmatrix} 1 & 1 \\ 1 & 2 \end{pmatrix}} |H_{-1}\rangle$.

Some distillation schemes for $|H_{\pm}\rangle$ are discussed in [13].

The planar region of qutrit state space spanned by convex mixtures of the eigenvectors of H is shown in Figure 7b.

Note that H^{-1} has eigenvalues $-i, 1, -1$. H^{-1} is in the same conjugacy class as H only because we are ignoring overall phases in our definition of the Clifford group.

Eigenvectors of $[[XV_{\hat{S}}]]$

$[[XV_{\hat{S}}]]$ includes the conjugacy classes $[XV_{\hat{S}}]$ and $[(XV_{\hat{S}})^{-1}]$. The eigenvectors for $XV_{\hat{S}}$ and its inverse were already studied in [35], and distillation routines for these states were studied in [14]. In terms of $\xi = e^{2\pi i/9}$, these can be written as

$$|XV_{\hat{S}}, \xi^7\rangle = \xi^8 |0\rangle + \xi |1\rangle + |2\rangle \quad (3.27)$$

$$|XV_{\hat{S}}, \xi^4\rangle = \xi^2 |0\rangle + \xi^7 |1\rangle + |2\rangle \quad (3.28)$$

$$|XV_{\hat{S}}, \xi\rangle = \xi^5 |0\rangle + \xi^4 |1\rangle + |2\rangle. \quad (3.29)$$

One can check that the different eigenvectors are related to each other by multiplication by Z . So there is one inequivalent magic state which we take to be

$$|XV_{\hat{S}}\rangle = \xi^5 |0\rangle + \xi^4 |1\rangle + |2\rangle. \quad (3.30)$$

3.2 Qutrit Clifford Eigenstates

We find that there are four inequivalent non-degenerate qutrit Clifford eigenstates,

$$|S\rangle, |H_+\rangle, |N_+\rangle \text{ and } |XV_{\hat{S}}\rangle. \quad (3.31)$$

In addition there are two families of degenerate Clifford eigenspaces:

$$|V_{-1}, 1; \alpha, \beta\rangle = \alpha |0\rangle + \beta (|1\rangle + |2\rangle) \quad (3.32)$$

$$|V_{\hat{S}}, \omega^2; \gamma, \delta\rangle = \gamma |1\rangle + \delta |2\rangle. \quad (3.33)$$

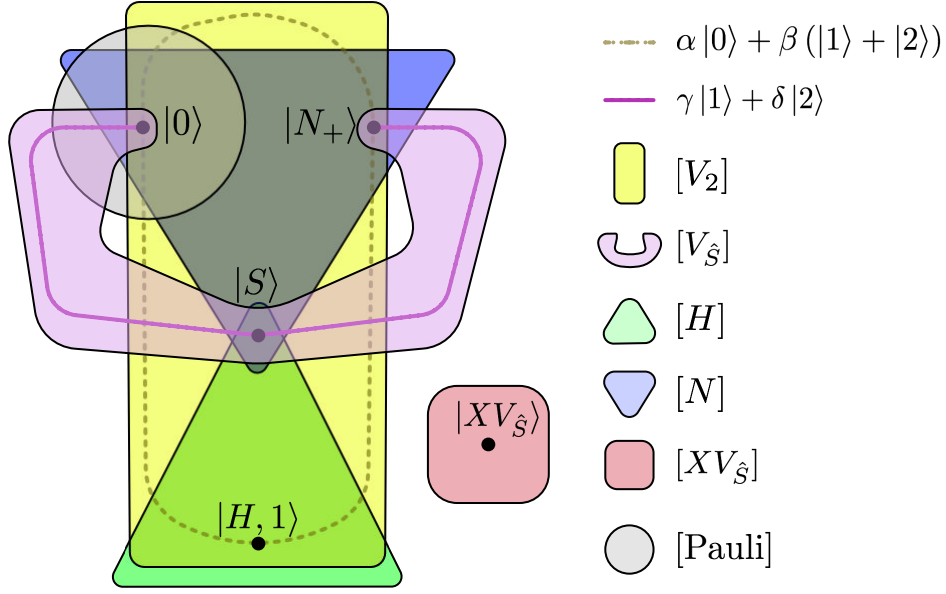


Figure 1: This diagram illustrates all inequivalent qutrit Clifford eigenstates, depicted as points, and their corresponding reduced conjugacy classes, depicted as colored regions. 1-parameter degenerate families of eigenstates are represented by curves.

The two degenerate eigenspaces $|V_{-1}, 1; \alpha, \beta\rangle$ and $|V_{\hat{S}}, \omega^2; \gamma, \delta\rangle$ only intersect at points equivalent to $|0\rangle$ and $|N_+\rangle$.

We depict all these candidate magic states via the (generalized) “hypergraph” in Figure 1. (This is reminiscent of the hypergraph construction of [60].) In this figure, the conjugacy classes of the Clifford group are represented by colored regions. Each non-degenerate, inequivalent eigenstate is depicted as a point, and each degenerate family of eigenstates is depicted as a line. An eigenstate of an operator A belonging to $[[A]]$ is contained within the region corresponding to $[[A]]$. Some magic states, such as $|S\rangle$ are contained in more than one region, as they are simultaneous eigenvectors of operators belonging to different conjugacy classes.

In the next sections, we discuss each of the candidate magic states in detail. This discussion is summarized in Table 1.

3.2.1 The Strange State $|S\rangle$

The state $|H, i\rangle$ is also known as the strange state $|S\rangle$, and was identified as one of the two states that maximize the mana in [23]. As illustrated from Figure 1, the strange state is an

State	Conjugacy Classes	Mana	Min(W_ρ)	Orbit
$ S\rangle$	$[[H]], [[V_{\hat{S}}]], [[V_{-1}]], [[N]]$	$\log \frac{5}{3} \approx 0.51$	-0.33	9
$ H_{\pm}\rangle$	$[[H]], [[V_{-1}]]$	$\log \left(\frac{1}{3} + \frac{2}{\sqrt{3}} \right) \approx 0.40$	-0.06	54
$ N_{+}\rangle$	$[[V_{\hat{S}}]], [[V_{-1}]], [[N]]$	$\log \left(\frac{5}{3} \right) \approx 0.51$	-0.17	36
$ XV_{\hat{S}}\rangle$	$[[XV_{\hat{S}}]]$	$\log \left(\frac{1}{3} \left(1 + 4 \cos \left(\frac{\pi}{9} \right) \right) \right) \approx 0.46$	-0.10	72

Table 1: **List of Non-Degenerate Qutrit Clifford Eigenstates:** For each state, we list the conjugacy classes it is an eigenvector of, its mana, its the most negative entry in its discrete Wigner function denoted as $\text{Min}(W_\rho)$, and the size of its orbit under the Clifford group (denoted as $|\text{Orbit}|$).

eigenstate of several reduced conjugacy classes, with the following eigenvalues:

$$V_{-1} |S\rangle = -1 |S\rangle \quad (3.34)$$

$$N |S\rangle = e^{\pi i/3} |S\rangle \quad (3.35)$$

$$V_H |S\rangle = i |S\rangle \quad (3.36)$$

$$V_{\hat{S}} |S\rangle = \omega^2 |S\rangle \quad (3.37)$$

The discrete Wigner function representation of $|S\rangle$ is particularly simple:

$$W_{u,v}(|S\rangle \langle S|) = \begin{cases} -1/3 & (u,v) = (0,0) \\ 1/6 & (u,v) \neq (0,0) \end{cases}. \quad (3.38)$$

It is depicted graphically in Figure 2a.

From this Wigner function, we see that the state $|S\rangle$ lies directly above the “center” of one facet of the Wigner polytope, and also maximally violates the contextuality inequality of [18]. Distillation of the $|S\rangle$ state therefore, has the theoretical potential to have the highest threshold to noise of all qutrit magic states, [20] although as argued in [50], the limit is unattainable by any finite distillation routine. In this sense, it is analogous to $|T\rangle$ states for qubits [1, 52].

The orbit of $|S\rangle$ under the full Clifford group contains 9 states, and its orbit under symplectic rotations is of size 1.

The mana of this state is $\log \frac{5}{3}$, which is maximal. [23] The Norell state, $|N_{+}\rangle$, also has maximal mana. However, the strange state has larger *thuma* [24] than the Norell state. So, from the perspective of magic as a resource, the strange state is the most magic qutrit state.

No magic state distillation routine that distills the strange state was known until very recently. [17]

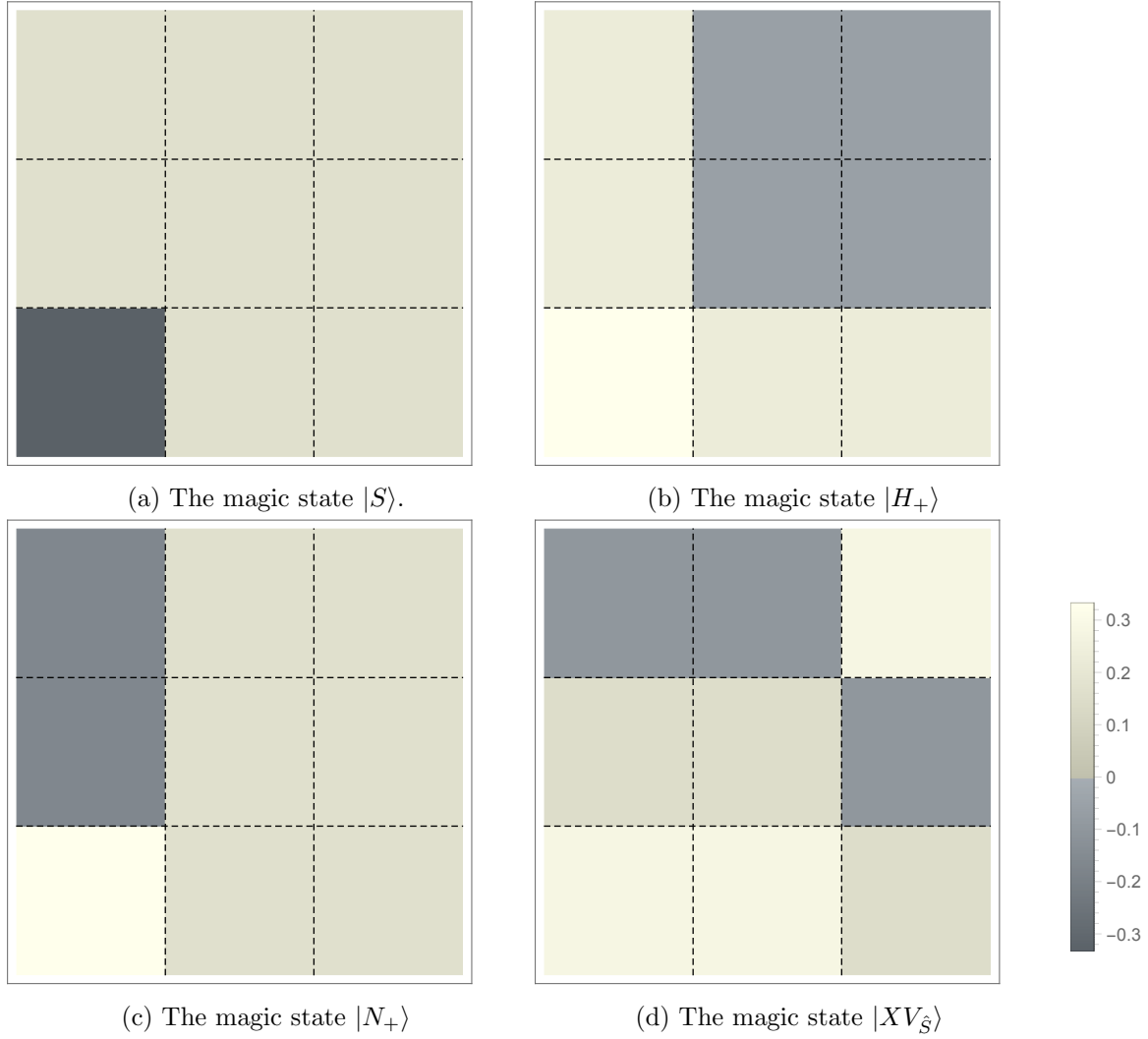


Figure 2: **Discrete Wigner functions of the four non-degenerate qutrit magic states**

3.2.2 The State $|H_+\rangle$

The state $|H_+\rangle$ is an eigenstate of the following operators:

$$V_{-1} |H_{\pm}\rangle = 1 |H_{\pm}\rangle \quad (3.39)$$

$$V_H |H_{\pm}\rangle = \pm |H_{\pm}\rangle \quad (3.40)$$

Its discrete Wigner function is given by

$$W_{u,v}(|H_+\rangle \langle H_+|) = \begin{pmatrix} W_{2,0} & W_{2,1} & W_{2,2} \\ W_{1,0} & W_{1,1} & W_{1,2} \\ W_{0,0} & W_{0,1} & W_{0,2} \end{pmatrix} = \begin{pmatrix} \frac{1}{12} (1 + \sqrt{3}) & \frac{1}{-6-6\sqrt{3}} & \frac{1}{-6-6\sqrt{3}} \\ \frac{1}{12} (1 + \sqrt{3}) & \frac{1}{-6-6\sqrt{3}} & \frac{1}{-6-6\sqrt{3}} \\ \frac{1}{3} & \frac{1}{12} (1 + \sqrt{3}) & \frac{1}{12} (1 + \sqrt{3}) \end{pmatrix} \quad (3.41)$$

and is depicted in Figure 2b.

The orbit of $|H_+\rangle$ under the full Clifford group contains 54 states, and its orbit under symplectic rotations contains 6 states. Its orbit under the quaternion subgroup of symplectic rotations contains 2 states; its orbit under two of the three Z_4 subgroups that do not contain H , each contain 2 states. Its orbit under the Z_3 and Z_6 subgroups each contain 3 states. It is an eigenstate of V_{-1} .

The mana of $|H_+\rangle$ is $\log\left(\frac{1}{3} + \frac{2}{\sqrt{3}}\right)$.

A distillation routine for $|H_+\rangle$ states, with only a linear reduction in noise, was presented in [13].

3.2.3 The Norell State $|N_+\rangle$

The state $|N_+\rangle$ is an eigenvector of the following Clifford operators:

$$V_{-1} |N\rangle = 1 |N_+\rangle \quad (3.42)$$

$$V_N |N_+\rangle = -e^{i\pi/3} |N_+\rangle. \quad (3.43)$$

Its discrete Wigner function is:

$$W_{u,v}(|N_+\rangle \langle N_+|) = \begin{pmatrix} -\frac{1}{6} & \frac{1}{6} & \frac{1}{6} \\ -\frac{1}{6} & \frac{1}{6} & \frac{1}{6} \\ \frac{1}{3} & \frac{1}{6} & \frac{1}{6} \end{pmatrix} \quad (3.44)$$

This is plotted in Figure 2c.

The orbit of this state under the Clifford group contains 36 states, and its orbit under the set of symplectic rotations contains 4 states. Its orbit under the quaternion subgroup contains 4 states, and its orbit under each of the Z_4 subgroups contain 2 states. Its orbit under the three (of four) Z_6 subgroups that do not contain N each contain 3 states. Its orbit under the three (of four) Z_3 subgroups that do not contain $V_{\hat{S}}$ each also contain 3 states.

Its mana is $\log\left(\frac{5}{3}\right)$, which is maximal. It was identified as a *Norell state* in [23]. However, as shown in [24], its thauma is less than that of the strange state, so it is not the most magic qutrit state.

A distillation routine with linear reduction in noise for the Norell state was found in [16]. A better distillation routine was recently discovered. [17]

3.2.4 The State $|XV_{\hat{S}}\rangle$

Its discrete Wigner function is:

$$W_{u,v}(|XV_{\hat{S}}\rangle \langle XV_{\hat{S}}|) = \frac{1}{9} \begin{pmatrix} 1 - 2 \cos\left(\frac{\pi}{9}\right) & 1 - 2 \cos\left(\frac{\pi}{9}\right) & 1 + 2 \cos\left(\frac{2\pi}{9}\right) \\ 1 + 2 \sin\left(\frac{\pi}{18}\right) & 1 + 2 \sin\left(\frac{\pi}{18}\right) & 1 - 2 \cos\left(\frac{\pi}{9}\right) \\ 1 + 2 \cos\left(\frac{2\pi}{9}\right) & 1 + 2 \cos\left(\frac{2\pi}{9}\right) & 1 + 2 \sin\left(\frac{\pi}{18}\right) \end{pmatrix} \quad (3.45)$$

This is plotted in Figure 2d.

The orbit of $|XV_{\hat{S}}\rangle$ under the Clifford group contains 72 states, and its orbit under the group of symplectic rotations contains 24 states.

Its mana is $\log\left(\frac{1}{3}\left(1 + 4\cos\left(\frac{\pi}{9}\right)\right)\right)$.

Distillation and state-injection schemes for this state were given in [14]. It is worth noting that the $|XV_{\hat{S}}\rangle$ state is equatorial, [14] and a single pure copy of this state can be used to implement the qutrit version of the $\pi/8$ gate [35, 61] without any chance of error via state injection.

3.2.5 Degenerate Eigenstates of V_{-1}

Let us parameterize the family of states $|2; \alpha, \beta\rangle$ via $\alpha = \cos \theta$ and $b = e^{i\phi} \sin \theta$. In terms of these variables, its mana is

$$\log\left(\frac{1}{6}\left(2\left(\left|\sin \theta \left(2\sqrt{2} \cos \theta \cos \phi + \sin \theta\right)\right| + \left|\sin \theta \left(\sin \theta - 2\sqrt{2} \cos \theta \sin\left(\frac{\pi}{6} - \phi\right)\right)\right| + \left|\sin \theta \left(\sin \theta - 2\sqrt{2} \cos \theta \sin\left(\phi + \frac{\pi}{6}\right)\right)\right| + 1\right) + |3 \cos 2\theta + 1|\right)\right). \quad (3.46)$$

This is plotted in Figure 3b. All states of the form $|2; a, b\rangle$ that maximize the mana are Clifford equivalent to $|N_+\rangle$ which has mana $\log \frac{5}{3}$. There are also local maxima at states Clifford equivalent to $|H_+\rangle$ and the state given by $\theta = \arctan(-\sqrt{2})/2 + \pi/2$, and $\phi = \pi/3$.

Some distillation schemes for the first family of states $|V_{-1}, 1; a, b\rangle$ were studied in [16].

3.2.6 Degenerate Eigenstates of $V_{\hat{S}}$

Let us parameterize the family of states $|V_{\hat{S}}; \gamma, \delta\rangle$ via $\gamma = \cos \psi$ and $\delta = e^{i\chi} \sin \psi$. In terms of these real variables, its discrete Wigner function is:

$$\frac{1}{3} \begin{pmatrix} -\sin 2\psi \cos(\chi - \pi/3) & \cos^2 \psi \sin^2 \psi \\ -\sin 2\psi \cos(\chi + \pi/3) & \cos^2 \psi \sin^2 \psi \\ \sin 2\psi \cos \chi & \cos^2 \psi \sin^2 \psi \end{pmatrix}. \quad (3.47)$$

Its mana is

$$\log\left(\frac{1}{3}\left(\left|\sin\left(\frac{\pi}{6} - \chi\right) \sin(2\psi)\right| + \left|\sin\left(\chi + \frac{\pi}{6}\right) \sin(2\psi)\right| + |\cos \chi \sin(2\psi)| + 3\right)\right). \quad (3.48)$$

This is plotted in Figure 3b. The states in the family $|V_{\hat{S}}; \gamma, \delta\rangle$ that maximize the mana are Clifford equivalent to either $|S\rangle = \frac{1}{\sqrt{2}}(|1\rangle - |2\rangle)$ or $|N_+\rangle = \frac{1}{\sqrt{2}}(|1\rangle + |2\rangle)$.

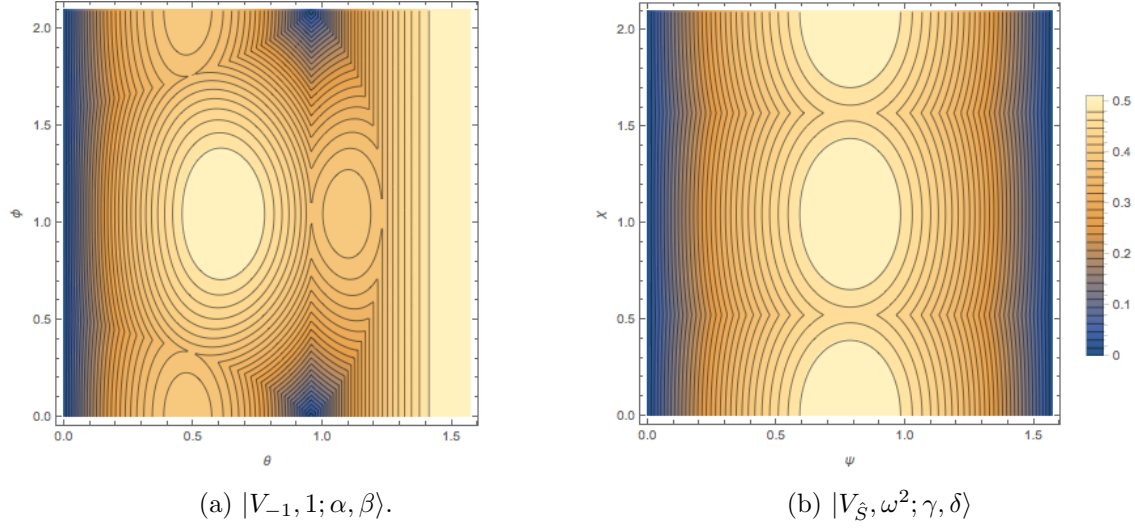


Figure 3: The mana of the two degenerate families of qutrit states, plotted as a function of the angular variables given in the text.

4 Eigenstates of Ququint Clifford Operators

We now turn to ququint magic states. We use similar notation as in the previous section, such as H and $V_{\hat{S}}$, for ququint Clifford operators and states. We hope that it is clear from context that all operators and states in this section are ququint operators and states.

4.1 Conjugacy Classes of the Single-Ququint Clifford group

There are 14 conjugacy classes of the single-ququint Clifford group. These are $[[I]]$, $[[\text{Pauli}]]$, and

$$[[V_{-1}]] = [V_{-1}] \quad (4.1)$$

$$[[V_{\hat{S}}]] = [V_{\hat{S}}], [V_{\hat{S}}^{-1}] \quad (4.2)$$

$$[[H]] = [H], \quad (4.3)$$

$$[[A]] = [V_{\hat{S}}H^2], [V_{\hat{S}}^2H^2], \quad (4.4)$$

$$[[B]] = [HV_{\hat{S}}], [(HV_{\hat{S}})^{-1}], \quad (4.5)$$

$$[[C]] = [XV_{\hat{S}}], [X^2V_{\hat{S}}], [XV_{\hat{S}}^{-1}], [X^2V_{\hat{S}}^{-1}], \quad (4.6)$$

These are grouped into 8 reduced conjugacy classes, with one reduced conjugacy class per row. $[Z]$ has 24 elements, $[V_{-1}]$ has 25 elements, $[V_{\hat{S}}]$ has 60 elements, $[H]$ has 750 elements, $[V_{\hat{S}}H^2]$ has 300 elements, $[HV_{\hat{S}}]$ has 500 elements, and $[XV_{\hat{S}}]$ has 120 elements.

Repeating the same types of calculations performed above for qutrits, we find a total of 8 inequivalent non-degenerate eigenstates, two 1-parameter families of degenerate eigenstates, and one 2-parameter family of degenerate eigenstates.

Eigenstates of $V_{-1}^{(5)}$

$V_{-1}^{(5)}$ has two degenerate families of eigenstates:

$$|V_{-1}^{(5)}, 1; \alpha, \beta, \gamma\rangle = \gamma |0\rangle + \alpha(|1\rangle + |4\rangle) + \beta(|2\rangle + |3\rangle) \quad (4.7)$$

$$|V_{-1}^{(5)}, 1; \alpha, \beta\rangle = \alpha(|1\rangle - |4\rangle) + \beta(|2\rangle - |3\rangle). \quad (4.8)$$

Eigenstates of $V_{\hat{S}}$

The eigenstates of $V_{\hat{S}}$ are

$$|V_{\hat{S}}, 1\rangle = |0\rangle \quad (4.9)$$

$$|V_{\hat{S}}, \omega_5^2; \alpha, \beta\rangle = \alpha |2\rangle + \beta |3\rangle \quad (4.10)$$

$$|V_{\hat{S}}, \omega_5^3; \alpha, \beta\rangle = \alpha |1\rangle + \beta |4\rangle. \quad (4.11)$$

The families $|V_{\hat{S}}, \omega_5^2\rangle$ and $|V_{\hat{S}}, \omega_5^3\rangle$ are related to each other by a Clifford transformation.

Eigenstates of H

The eigenstates of H are:

$$|H, -1\rangle = (10 - 2\sqrt{5})^{-1/2} \left((1 - \sqrt{5}) |0\rangle + |1\rangle + |2\rangle + |3\rangle + |4\rangle \right) \quad (4.12)$$

$$|H, \pm i\rangle = \frac{1}{2} \left(\sqrt{1 \mp \chi} (|1\rangle - |4\rangle) + \sqrt{1 \pm \chi} (|2\rangle - |3\rangle) \right) \quad (4.13)$$

$$|H, 1; \alpha, \beta\rangle = (1 + \sqrt{5})/2 (\alpha - \beta) |0\rangle + \alpha (|1\rangle + |4\rangle) + \beta (|2\rangle + |3\rangle) \quad (4.14)$$

where $\chi = \sqrt{\frac{1}{10} (5 + \sqrt{5})}$. $|H, \pm i\rangle$ are related to each other via a Clifford transformation. $|H, -1\rangle$ can be mapped to a member of $|H, 1\rangle$ via a Clifford transformation.

Eigenstates of $[[A]]$

The eigenstates of $A = V_{\hat{S}} H^2$ are:

$$|A, 1\rangle = |0\rangle \quad (4.15)$$

$$|A, \pm \omega_5^2\rangle = \frac{1}{\sqrt{2}} (|2\rangle \pm |3\rangle) \quad (4.16)$$

$$|A, \pm \omega_5^3\rangle = \frac{1}{\sqrt{2}} (|1\rangle \pm |4\rangle). \quad (4.17)$$

$|A_+\rangle \equiv |A, \omega_5^2\rangle$ and $|A, \omega_5^3\rangle$ are related to each other by a Clifford transformation. $|A_-\rangle \equiv |A, -\omega_5^2\rangle$ and $|A, -\omega_5^3\rangle$ are also related to each other by a Clifford transformation.

Eigenstates of $[[B]]$

The reduced conjugacy class of $B = HV_{\hat{S}}$ also contains the operator $B' = KBK^{-1}$, where $K = XV \begin{pmatrix} 1 & 2 \\ 2 & 0 \end{pmatrix}$. The unnormalized eigenvectors of B' , which are all real and simpler to write

down than the eigenvectors of B , can be presented as:

$$|B', -1\rangle = \frac{1}{2} \left(3 + \sqrt{5} \right) |0\rangle + |1\rangle + |2\rangle + |3\rangle + |4\rangle \quad (4.18)$$

$$|B', e^{\frac{\pm 2\pi i}{3}}\rangle = \frac{1}{4} \eta_{\pm} (|1\rangle - |4\rangle) + |2\rangle - |3\rangle \quad (4.19)$$

$$|B', -e^{\frac{\pm 2\pi i}{3}}\rangle = \kappa_{\pm} |0\rangle - \kappa_{\pm}^2 / 4 (|1\rangle + |4\rangle) + |2\rangle + |3\rangle. \quad (4.20)$$

where $\eta_{\pm} = \left(\mp \sqrt{30 - 6\sqrt{5}} + \sqrt{5} - 3 \right)$ and $\kappa_{\pm} = \frac{1}{2} \left(\pm \sqrt{6(5 + \sqrt{5})} - \sqrt{5} - 3 \right)$. Of these states, $|B', -e^{\frac{\pm 2\pi i}{3}}\rangle$ are equivalent to each other by a Clifford transformation, and $|B', e^{\frac{\pm 2\pi i}{3}}\rangle$ are equivalent to each other by a Clifford transformation.

In Figure 5, we plot Wigner functions for the eigenvectors of B not B' , because the symmetry of B is easier to visualize in discrete phase space.

Eigenstates of $[[C]]$

The reduced conjugacy class $[[C]]$ includes the operator $XV_{\hat{S}}$. Its eigenstates were found in [35, 13]. These are:

$$|C, 1\rangle = |0\rangle + |1\rangle + \omega_5^3 |2\rangle + |3\rangle + \omega_5^2 |4\rangle \quad (4.21)$$

$$|C, \omega_5^n\rangle = (Z^\dagger)^n |C, 1\rangle. \quad (4.22)$$

All are related to each other by a Clifford transformation.

4.2 Quint Clifford Eigenstates

In summary, we have nine inequivalent non-degenerate eigenstates (including $|0\rangle$), 3 one-parameter families of degenerate states, and 1 two-parameter family of degenerate states. These are shown in Figure 4. Colored regions correspond to reduced conjugacy classes, and eigenstates of conjugacy classes are contained in their corresponding regions, as in Figure 1. Degenerate families of eigenstates are shown as lines.

The only intersections of $|V_{\hat{S}}, \omega^2\rangle$ and $|H, 1\rangle$ are Clifford-equivalent to $|0\rangle$. The only intersections of $|V_{\hat{S}}, \omega^2\rangle$ and $|V_{-1}, \omega^2\rangle$ are Clifford-equivalent to $|A_2\rangle$. $|H, 1\rangle$ and $|V_{-1}\rangle$ have no intersections.

We plot the discrete Wigner function of the eight non-degenerate non-stabilizer states in Figure 5. For each non-degenerate state, we list the reduced conjugacy classes it is an

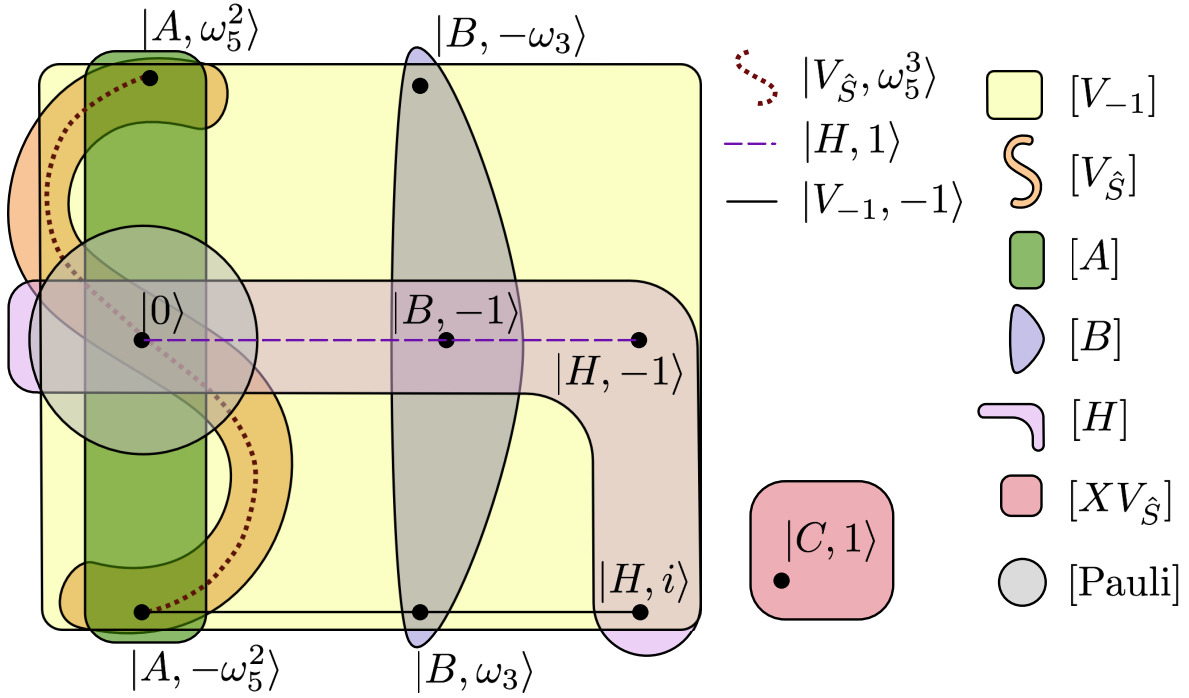


Figure 4: This diagram illustrates all inequivalent ququint Clifford eigenstates, depicted as points, and their corresponding reduced conjugacy classes, depicted as colored regions. 1-parameter degenerate families of eigenstates are represented by curves. The 2-parameter degenerate family of states $|V_{-1}, 1\rangle$ is not pictured.

eigenvector of, the mana, and the size of its orbit under the Clifford group in Table 2. We plot the mana for each of the one parameter families of degenerate eigenstates in Figure 6.

Based on a numerical search, we find that the maximal mana for any ququint state is

$$\mathcal{M}_5 = \sinh^{-1} \left(3 + \sqrt{5} \right) - \log(5), \quad (4.23)$$

which is attained by the states Clifford equivalent to $|B', -e^{\frac{2\pi i}{3}}\rangle$. We are not sure if there are any other states which have the same mana, but they do not appear to be any. Therefore we conjecture that $|B', -e^{\frac{\pm 2\pi i}{3}}\rangle$ is the most magic ququint state. The most symmetric Clifford eigenstate, which we define as that eigenstate with the smallest orbit under the Clifford group is $|B, -1\rangle$. Unlike the qutrit case, the most magic state is not the most symmetric. Also, as can be seen from this Figure, there is no ququint Clifford eigenstate with exactly one negative entry in the Wigner function.

Magic state distillation routines for the state $|C, 1\rangle$ were constructed in [14, 15]. To our knowledge, magic state distillation routines for the other ququint magic states have not yet been constructed.

State	Conjugacy Classes	Mana	Min(W_ρ)	Orbit
$ H, i\rangle$	$[[H]], [[V_{-1}]]$	$\log \frac{1}{5} \left(2\sqrt{5} + 2\sqrt{5} + 3 \right) \approx .605$	-.20	750
$ H, -1\rangle$	$[[H]], [[V_{-1}]]$	$\log \frac{9}{5} \approx .588$	-.05	375
$ B, -1\rangle$	$[[B]], [[H]], [[V_{-1}]]$	$\log \left(\frac{1}{5} + \frac{4}{\sqrt{5}} \right) \approx .688$	-.04	250
$ B, -e^{\frac{2\pi i}{3}}\rangle$	$[[B]], [[V_{-1}]]$	$\sinh^{-1} \left(3 + \sqrt{5} \right) - \log(5) \approx .748$	-.09	500
$ B, e^{\frac{2\pi i}{3}}\rangle$	$[[B]], [[V_{-1}]]$	$\log \frac{\sqrt{15+6\sqrt{5}}+4}{5} \approx .624$	-.20	500
$ A, -\omega_5^2\rangle$	$[[A]], [[V_{\hat{S}}]], [[V_{-1}]]$	$\log \left(\frac{6}{5} + \frac{1}{\sqrt{5}} \right) \approx .499$	-.20	300
$ A, \omega_5^2\rangle$	$[[A]], [[V_{\hat{S}}]], [[V_{-1}]]$	$\log \left(\frac{6}{5} + \frac{1}{\sqrt{5}} \right) \approx .499$	-.16	300
$ C, 1\rangle$	$[[C]]$	$\log \left(1 + \frac{2}{\sqrt{5}} \right) \approx .634$	-.09	600

Table 2: **List of Non-Degenerate Ququint Clifford Eigenstates**– For each state, we list the conjugacy classes it is an eigenvector of, its mana, its the most negative entry in its discrete Wigner function (denoted as Min(W_ρ), and the size of its orbit under the Clifford group (denoted as |Orbit|).

5 Twirling Schemes

To avoid the complexities of the possible noise in an initial noisy magic state, it is conventional to “twirl” the undistilled resource state into a density matrix of a simpler form prior to distillation by randomly applying one or more Clifford operators that have the target magic state as an eigenvector.

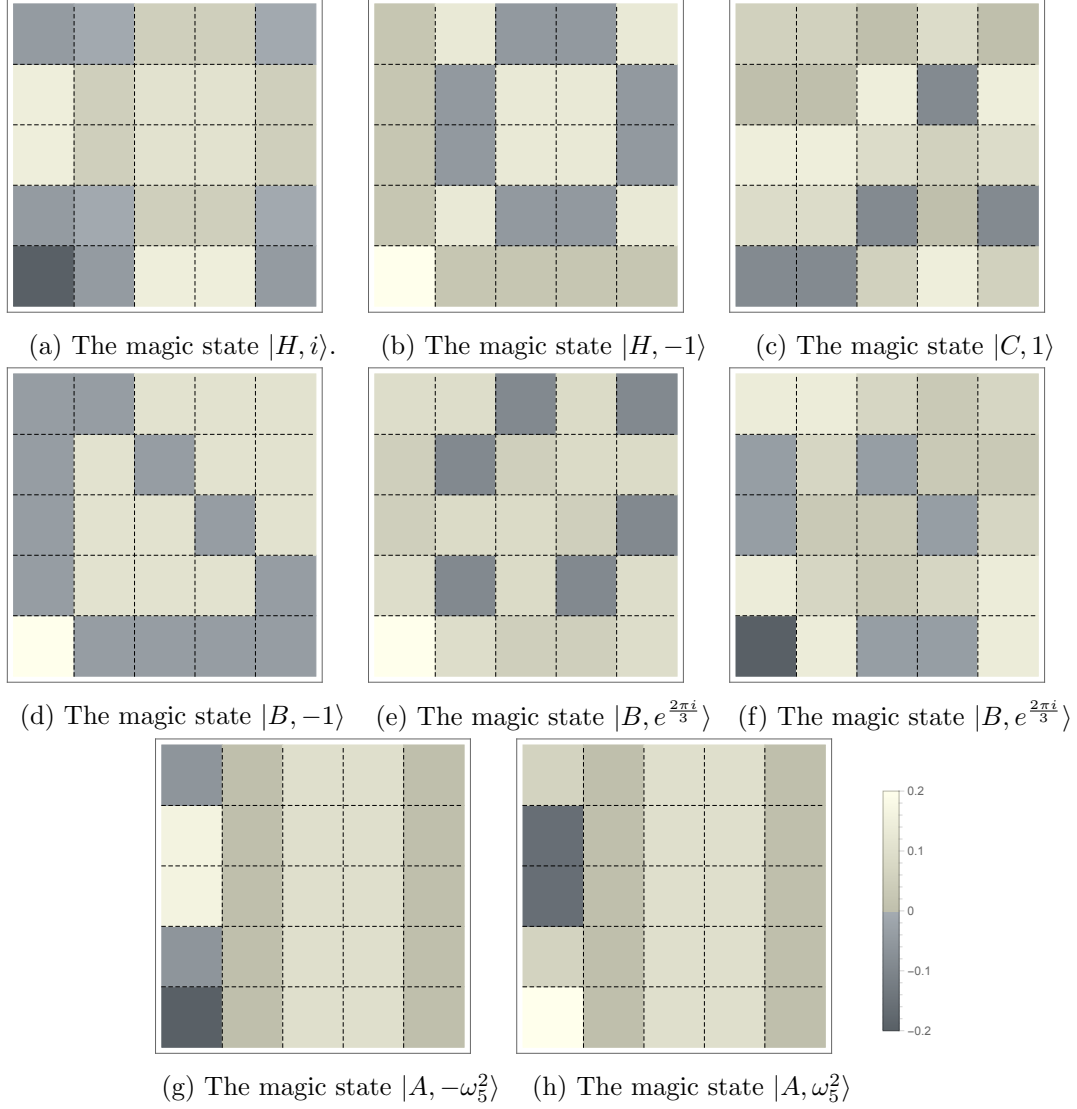


Figure 5: **Discrete Wigner functions of the 8 non-degenerate quqint Clifford eigenstates**

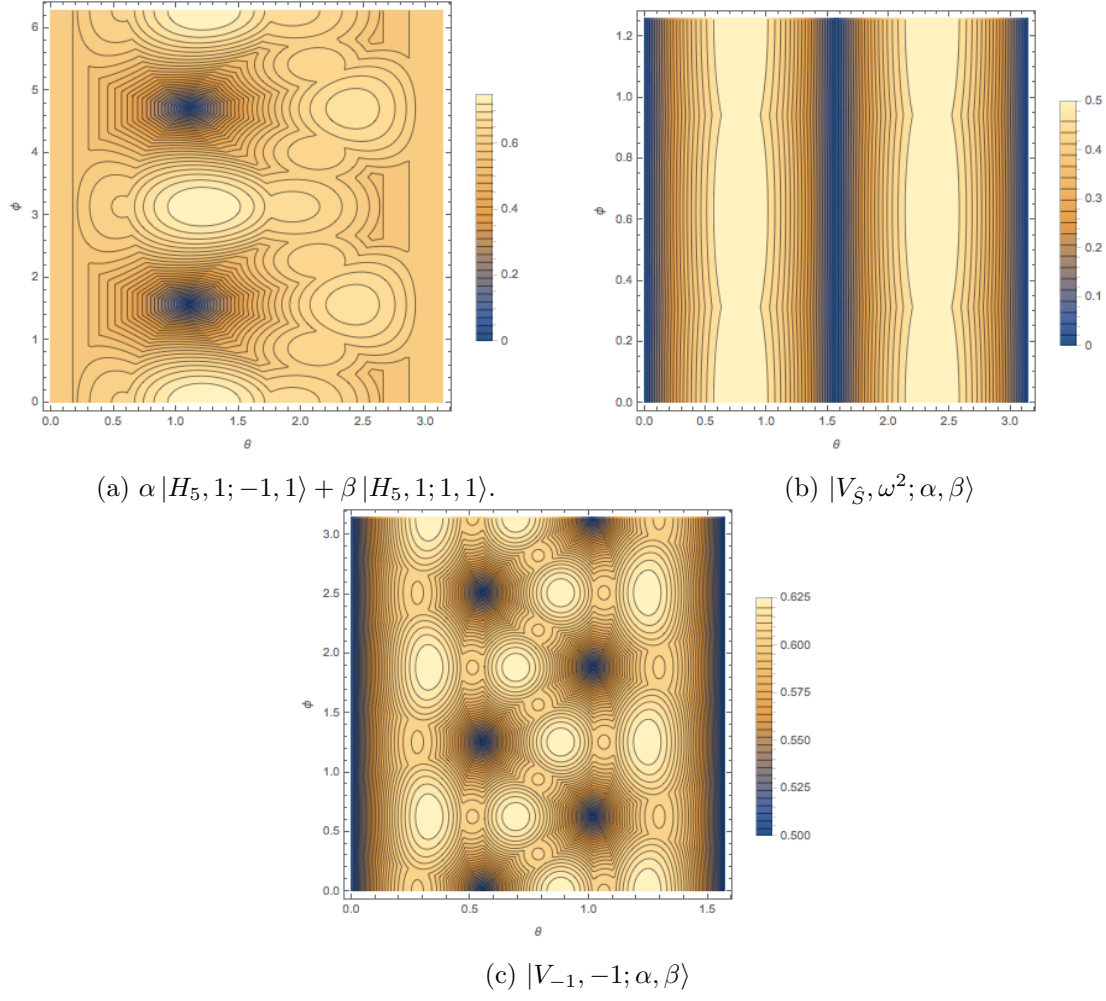


Figure 6: The mana of each of the one-complex-parameter degenerate families of ququint Clifford eigenstates, with $\alpha = \cos \frac{\theta}{2}$ and $\beta = e^{i\phi} \sin \frac{\theta}{2}$. θ is the horizontal axis, and ϕ is the vertical axis.

State	Generators	Order	Group
$ S\rangle$	$\langle H, V_{\hat{S}} \rangle$	24	$SL(2, Z_3)$
$ H_+\rangle$	$\langle H \rangle$	4	C_4
$ N_+\rangle$	$\langle N \rangle$	6	C_6
$ XV_{\hat{S}}\rangle$	$\langle XV_{\hat{S}} \rangle$	3	C_3

Table 3: **The Stabilizing subgroup of the Clifford group for each qutrit magic state.** We list the largest subgroup of the Clifford group that stabilizes each magic state in the table above. The columns specify: the list of generators, order of the group and the name of the group.

For qubits, it was possible to restrict all forms of noise to depolarizing noise. This is not true in general for qudits. Generically, we expect twirling to reduce the number of parameters specifying the input qudit density matrices from $d^2 - 1$, to $d - 1$. This is not always the case, for magic states which are eigenstates of multiple conjugacy classes, we may be able to reduce the number of parameters further, and if a conjugacy class has degenerate eigenvectors, we may require additional parameters.

The diagram in Figure 1 can be used to determine the inequivalent twirling schemes that may be applied before distilling any given magic state. More generally, any subgroup of the Clifford group defines a twirling scheme.

Define the *stabilizing subgroup of the Clifford group* for state $|M\rangle$ as set of elements of the Clifford group for which $|M\rangle$ as an eigenvector. Here, we say C “stabilizes” $|M\rangle$ when $C|M\rangle = \lambda|M\rangle$, for any λ .) The stabilizing subgroup of the Clifford group provides a natural scheme for twirling.

5.1 Qutrits

We present the largest stabilizing subgroup of the Clifford group for each state in Table 3. We illustrate the twirling schemes for each state in detail below, which are also pictured in Figure 7.

5.1.1 Twirling Schemes for H States

To distill eigenstates of H , one can randomly apply the Clifford operator H which will restrict our input state to the plane defined by $|S\rangle\langle S|$, $|H_+\rangle\langle H_+|$, and $|H_-\rangle\langle H_-|$ given in Figure 7b.

$$\rho_H(\epsilon_1, \epsilon_2) = (1 - \epsilon_1 - \epsilon_2) |S\rangle\langle S| + \epsilon_1 |H_1\rangle\langle H_1| + \epsilon_2 |H_{-1}\rangle\langle H_{-1}|. \quad (5.1)$$

If we want to distill $|H_+\rangle$ state, there is no further twirling possible.

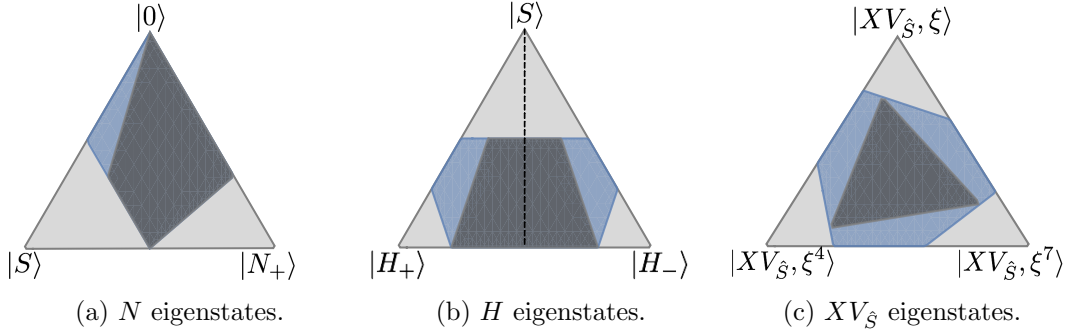


Figure 7: Noisy qutrit magic states can be twirled to lie in the planar slice of qutrit state space formed by the non-degenerate eigenvectors of each Clifford conjugacy class. Noisy strange states, can be further twirled to lie on the dashed line. The Wigner polytope is pictures as a blue region, which contains the Stabilizer polytope as a dark gray region. The centre of each equilateral triangle is the maximally mixed state.

If we wish to distill $|S\rangle$ states, we can further twirl to restrict input and output states to lie in a line in qudit state space. The states $|H_+\rangle$ and $|H_-\rangle$ are interchanged by a Clifford operator that preserves $|S\rangle$, we can further twirl by randomly applying this Clifford operator. The final result is equivalent to applying a random symplectic rotation $V_{\hat{F}}$. Input states are then restricted to the line which joins $|S\rangle \langle S|$ to the maximally mixed state, shown as a dashed line in Figure 7b, and can be parameterized as follows:

$$\begin{aligned}
\rho_S(\epsilon/2, \epsilon/2) &= (1 - \epsilon) |S\rangle \langle S| + \epsilon \frac{(|H_1\rangle \langle H_1| + |H_{-1}\rangle \langle H_{-1}|)}{2} \\
&= (1 - \delta) |S\rangle \langle S| + \delta \frac{\mathbf{1}}{3},
\end{aligned} \tag{5.2}$$

where $\delta = \frac{3}{2}\epsilon$ is the depolarizing noise rate.

For all other magic states, it appears that twirling can only restrict the input state to lie in a plane. So the scheme given above is unique to $|S\rangle$.

5.1.2 Twirling Schemes for N States

An alternative twirling scheme is to randomly apply the N operator, so that states are restricted to the plane defined by its eigenvectors given in Figure 7a. This can be used to distill $|S\rangle$ or $|N_+\rangle$ states. A density matrix in this plane can be expressed as:

$$\rho_N(\epsilon_1, \epsilon_2) = (1 - \epsilon_1 - \epsilon_2) |N_+\rangle \langle N_+| + \epsilon_1 |0\rangle \langle 0| + \epsilon_2 |S\rangle \langle S|. \tag{5.3}$$

For stabilizer codes used with this twirling scheme, N should be a transversal operator.

5.1.3 Twirling Schemes for $XV_{\hat{S}}$ States

A third twirling scheme is to randomly apply the $XV_{\hat{S}}$ operator, so that states are restricted to the plane defined by its eigenvectors given in Figure 7c, which is useful for distilling $|XV_{\hat{S}}\rangle$ states. A density matrix in this plane can be expressed as,

$$\rho_{XV_{\hat{S}}}(\epsilon_1, \epsilon_2) = (1 - \epsilon_1 - \epsilon_2) |XV_{\hat{S}}\rangle \langle XV_{\hat{S}}| + \epsilon_1 |XV'_{\hat{S}}\rangle \langle XV'_{\hat{S}}| + \epsilon_2 |XV''_{\hat{S}}\rangle \langle XV''_{\hat{S}}|. \quad (5.4)$$

where $|XV'_{\hat{S}}\rangle$ and $|XV''_{\hat{S}}\rangle$ are the other eigenstates of $XV_{\hat{S}}$.

For stabilizer codes used with this twirling scheme, $XV_{\hat{S}}$ should be a transversal operator.

5.1.4 Twirling Schemes for Degenerate Families of States

For the degenerate families of states $|V_{\hat{S}}, \omega^2\rangle$, we can apply $V_{\hat{S}}$ a random number of times. The resulting space of density matrices will be 4-dimensional: 3-real parameters for the “Bloch sphere” of degenerate $|V_{\hat{S}}, \omega^2\rangle$ states, and additional parameter for the state $|0\rangle$. Similar comments apply for distilling, the states $|V_{-1}, 1\rangle$.

Explicitly, after randomly applying $V_{\hat{S}}$, any density matrix can be put in the form,

$$\rho(x, y, z, \epsilon) = (1 - \epsilon) \frac{1}{2} (|1\rangle \langle 1| + |2\rangle \langle 2| + x\Sigma_1 + y\Sigma_2 + z\Sigma_3) + \epsilon |0\rangle \langle 0| \quad (5.5)$$

where

$$\Sigma_1 = |1\rangle \langle 2| + |2\rangle \langle 1|, \quad \Sigma_2 = -i |1\rangle \langle 2| + i |2\rangle \langle 1|, \quad \Sigma_3 = |1\rangle \langle 1| - |2\rangle \langle 2|. \quad (5.6)$$

After randomly applying V_{-1} , any density matrix can be put in the form,

$$\tilde{\rho}(x, y, z, \epsilon) = (1 - \epsilon) \frac{1}{2} (|0\rangle \langle 0| + |N_+\rangle \langle N_+| + x\tilde{\Sigma}_1 + y\tilde{\Sigma}_2 + z\tilde{\Sigma}_3) + \epsilon |S\rangle \langle S| \quad (5.7)$$

where

$$\tilde{\Sigma}_1 = |0\rangle \langle N_+| + |N_+\rangle \langle 0|, \quad \tilde{\Sigma}_2 = -i |0\rangle \langle N_+| + i |N_+\rangle \langle 0|, \quad \tilde{\Sigma}_3 = |0\rangle \langle 0| - |N_+\rangle \langle N_+|. \quad (5.8)$$

5.2 Ququints

We present the largest stabilizing subgroup of the Clifford group for each ququint magic state in Table 4. These translate into twirling schemes in a straightforward way. Most of the schemes result in spaces with 4 or more parameters. However, the two cases of $|H, -1\rangle$ and $|B', -1\rangle$, give rise to smaller spaces after twirling, as we discuss below.

5.2.1 Twirling Scheme for the State $|H, -1\rangle$

We first randomly apply H to restrict ourselves to mixtures of $|H, \pm i\rangle$, $|H, -1\rangle$ and $|H, 1; \alpha, \beta\rangle$. This is a 6-parameter space.

State	Generators	Order	Group
$ H_i\rangle$	$\langle H \rangle$	4	C_4
$ H, -1\rangle$	$\langle H, H' \rangle$	8	Quaternion
$ B, -1\rangle$	$\langle B, H' \rangle$	12	Dicyclic ₃
$ B, -\omega_3^2\rangle$	$\langle B \rangle$	6	C_6
$ B, +\omega_3^2\rangle$	$\langle B \rangle$	6	C_6
$ A, -\omega^2\rangle$	$\langle A \rangle$	10	C_{10}
$ A, \omega^2\rangle$	$\langle A \rangle$	10	C_{10}
$ C\rangle$	$\langle XV_{\hat{S}} \rangle$	5	C_5

Table 4: **The stabilizing subgroup of the Clifford group for each non-degenerate ququint magic state.** We list the largest subgroup of the Clifford group that stabilizes each ququint magic state in the table above. The columns specify: the list of generators, order of the group and the name of the group.

The operator

$$H' = V \begin{pmatrix} 0 & 2 \\ 2 & 0 \end{pmatrix}, \quad (5.9)$$

is in the same conjugacy class as $[[H]]$. Together H and H' generate a non-abelian group of 8 elements, isomorphic to the quaternion group:

$$\text{Quaternion} = \langle H, H' \mid H^4 = 1, H'^2 = H^2, HH'H = H' \rangle. \quad (5.10)$$

The state $|H, -1\rangle$ is also an eigenstate of H' with eigenvalue -1 . H' acts on the other eigenstates of H as follows:

$$H' |H, +i\rangle = |H, -i\rangle, \quad H' |H, 1; 1, 1\rangle = |H, 1; 1, 1\rangle, \quad H' |H, 1; 1, -1\rangle = -|H, 1; 1, -1\rangle. \quad (5.11)$$

Thus by randomly applying H then H' , we obtain the three-parameter family of density matrices,

$$\begin{aligned} \rho = & (1 - \epsilon_1 - \epsilon_2 - \epsilon_3) |H, -1\rangle \langle H, -1| + \epsilon_1 |H, 1; 1, 1\rangle \langle H, 1; 1, 1| \\ & + \epsilon_2 |H, 1; 1, -1\rangle \langle H, 1; 1, -1| + \epsilon_3 \rho_i, \end{aligned} \quad (5.12)$$

where,

$$\rho_i = \frac{1}{2} (|H, +i\rangle \langle H, +i| + |H, -i\rangle \langle H, -i|). \quad (5.13)$$

This region is shown in Figure 8.

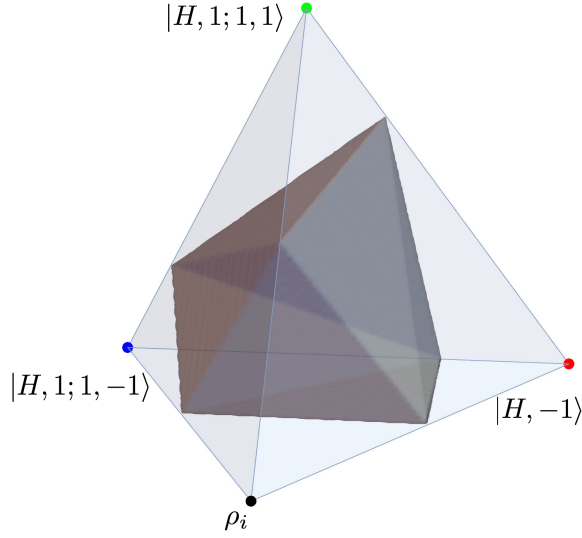


Figure 8: Noisy ququint $|H, -1\rangle$ states can be twirled to lie in the 3-dimensional convex mixture of states defined by Equation (5.12), depicted as a light-blue tetrahedron. The gray polytope inside is the Wigner polytope. The stabilizer polytope is not pictured.

5.2.2 Twirling Scheme for the State $|B', -1\rangle$

The state $|B, -1\rangle$ is an eigenvector of both B and H' . Together B and H' generate a non-abelian group of 12 elements known as the dicyclic group of order 12, sometimes written as Dicyclic_3 . It can be presented as:

$$\text{Dicyclic}_3 = \langle B, H' \mid B^6 = 1, H'^2 = B^3, H'^{-1}BH' = B^{-1} \rangle. \quad (5.14)$$

H' acts on the other eigenstates of B $|B, \pm\omega_3^2\rangle$ and $|B, \pm\omega_3^3\rangle$, as follows:

$$H' |B, +\omega^3\rangle = |B, +\omega^2\rangle, \quad H' |B, -\omega^3\rangle = |B, -\omega^2\rangle. \quad (5.15)$$

By randomly applying B , we are left with the four parameter family of convex combinations of $|B, -1\rangle$, $|B, \pm\omega_3^2\rangle$ and $|B, \pm\omega_3^3\rangle$. We then apply H' randomly to restrict our space to the two-parameter family of density matrices given by:

$$\rho_{B,-1}(\epsilon_+, \epsilon_-) = (1 - \epsilon_+ - \epsilon_-) |B, -1\rangle \langle B, -1| + \epsilon_+ \frac{1}{2} \rho_+ + \epsilon_- \rho_-. \quad (5.16)$$

Here, $\rho_{\pm} = \frac{1}{2} (|B, \pm\omega^2\rangle \langle B, \pm\omega^2| + |B, \pm\omega^3\rangle \langle B, \pm\omega^3|)$. This is shown in Figure 9.

6 Uniqueness of the Qutrit Strange State

As reviewed above the qutrit strange state has several interesting properties. The qutrit strange state is identified as the most magic qutrit state, by virtue of its maximal mana

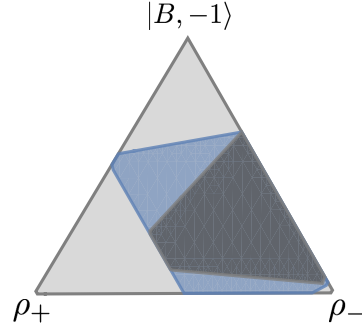


Figure 9: Noisy ququint $|B, -1\rangle$ states can be twirled to lie in the convex region defined by Equation (5.16), depicted as a light gray triangle. The dark blue region inside the triangle is the Wigner polytope, and the dark gray region is the stabilizer polytope.

and thauma. The qutrit strange state is also, in principle, maximally robust to polarizing noise. From the point of view of Clifford symmetries, the strange state is also distinguished as simultaneous eigenvector of all symplectic rotations. As such, it has a particularly simple discrete Wigner function, from which we see that it lies directly above the centre of a single facet of the Wigner polytope.

Does an analogue of the qutrit strange state exist for qudits of higher p that simultaneously possesses all these properties? In any dimension, one can determine states that maximize the mana, and also determine states that are maximally robust to depolarizing noise; however, and at least for $p = 5$, the states that maximize the mana are not equivalent to states that are maximally robust to depolarizing noise. One can also ask, does there exist a simultaneous eigenvector of all symplectic rotations for qudits of any other odd prime dimension d ?

Theorem 1. *There is no pure state that is a simultaneous eigenvector of all symplectic rotation, for qudits of odd prime dimension $d > 3$.*

Proof. A (non-stabilizer) eigenvector of all symplectic rotations must be an eigenvector of the generators of symplectic rotations H and $V_{\hat{S}}$. It is easy to see that there is no simultaneous eigenvector of $V_{\hat{S}}$ and H for odd prime $p > 3$.

$V_{\hat{S}}$ is diagonal in the computational basis. Its eigenvalues are $\lambda_i = \omega^{2^{-1}q_i}$ where q is any quadratic residue mod p , i.e., any element of \mathbb{Z}_p such that $q \equiv t^2 \pmod{p}$ for some t . There $(p+1)/2$ such quadratic residues, including 0. The eigenvector corresponding to $q = 0$ is $|0\rangle$ which is non-degenerate. The remaining $(p-1)/2$ quadratic residues each have two-dimensional degenerate eigenspaces of the form:

$$|V_{\hat{S}}, \omega^{2^{-1}q} = \alpha, \beta\rangle = \alpha |t\rangle + \beta |-t\rangle \quad (6.1)$$

where t and $-t$ are the two solutions to the equation $t^2 \equiv q \pmod{p}$.

If a simultaneous eigenvector of H and $V_{\hat{S}}$ exists, then $|V_{\hat{S}}, \omega^{2^{-1}q}; \alpha, \beta\rangle$ must be an eigenvector of H for some $q \neq 0$ and some choice of α and β . Let us see that this cannot be the case.

$$H |V_{\hat{S}}, \omega^{2^{-1}q}; \alpha, \beta\rangle = \sum_j (\alpha \omega^{jt} + \beta \omega^{-jt}) |j\rangle. \quad (6.2)$$

For $|V_{\hat{S}}, \omega^{2^{-1}q}; \alpha, \beta\rangle$ to be an eigenvector of H the coefficient of $|0\rangle$ must vanish in the above expression. This means that $\alpha = -\beta$. If $d > 3$, then there exists another $k \neq 0, \pm t$, such that the coefficient of $|k\rangle$ must also vanish in equation (6.2). This implies that $\alpha (\omega^{kt} - \omega^{-kt}) = 2i\alpha \sin(2\pi kt/p) = 0$, which means $\alpha = 0$ and no simultaneous eigenvector of H and $V_{\hat{S}}$ exists. \square

Our interpretation of this result is that the qutrit strange state is distinguished not only as both the most symmetric and magic qutrit state, but also the most symmetric of all qudit magic states.

Note that there are mixed states, other than the maximally mixed state, which are preserved by all symplectic rotations. Let ρ_S be an equal mixture of all stabilizer states without support on the phase space point $A_{0,0}$. (This excludes 1 basis vector from each of the $d+1$ mutually unbiased bases.) ρ_S has discrete Wigner function given by:

$$W_{u,v}(\rho) = \begin{cases} 0 & (u,v) = (0,0) \\ \frac{1}{p^2-1} & (u,v) \neq (0,0) \end{cases}. \quad (6.3)$$

Clearly, this Wigner function is preserved by all symplectic rotations.

Since the space of pure qudit density matrices is $2p-2$ -dimensional, and the space of all qutrit density matrices is p^2-1 -dimensional, most points at the boundary of qudit state space are not pure density matrices. Hence, there is no reason to expect the state directly above the centre of a face of the Wigner polytope to be a pure state, and the above argument shows that, for $p > 3$, it is not a pure state.

The absence of a state directly above a facet of the Wigner polytope does not mean that there are no states which maximally violate the contextuality inequality of [18]. There is always a conjugacy class $[[V_{-1}]]$, corresponding to $\begin{pmatrix} -1 & 0 \\ 0 & -1 \end{pmatrix} \in SL(2, Z_d)$. V_{-1} can be written as

$$V_{-1} = \sum_{k=0}^{p-1} |-k\rangle \langle k|. \quad (6.4)$$

Its eigenvalues are 1, which has degeneracy $(p+1)/2$, and -1 , which has degeneracy $(p-1)/2$. The corresponding eigenvectors were studied in [20]:

$$\begin{aligned} |V_1, 1; \alpha_i\rangle &= \alpha_0 |0\rangle + \sum_{j=1}^{(p-1)/2} \frac{\alpha_j}{\sqrt{2}} (|j\rangle + |-j\rangle) \\ |V_1, -1; \beta_i\rangle &= \sum_{j=1}^{(p-1)/2} \frac{\beta_j}{\sqrt{2}} (|j\rangle - |-j\rangle). \end{aligned}$$

From the results of [18], the minimum entry of the (normalized) discrete Wigner function is $-1/p$. Since $A_{00} = V_{-1}$, this shows that there are always Clifford eigenstates that attain this minimum value, i.e., that maximally violate the contextuality inequality. As emphasized in [20], these states have the potential to be distilled with the largest threshold to depolarizing noise.

Acknowledgements

SP would like to thank Rev. Prof. PS Satsangi for guidance. This research is supported in part by a DST INSPIRE Faculty award, DST-SERB Early Career Research Award (ECR/2017/001023) and MATRICS grant (MTR/2018/001077).

References

- [1] S. Bravyi and A. Kitaev, “Universal quantum computation with ideal Clifford gates and noisy ancillas,” *Phys. Rev. A* **71** (Feb, 2005) 022316, [arXiv:quant-ph/0403025](#).
- [2] E. Knill, “Quantum computing with realistically noisy devices,” *Nature* **434** (Mar, 2005) 39–44, [quant-ph/0410199](#).
- [3] E. T. Campbell, B. M. Terhal, and C. Vuillot, “Roads towards fault-tolerant universal quantum computation,” *Nature* **549** (Sept., 2017) 172–179, [1612.07330](#).
- [4] B. W. Reichardt, “Quantum Universality from Magic States Distillation Applied to CSS Codes,” *Quantum Information Processing* **4** (Aug, 2005) 251–264.
- [5] B. W. Reichardt, “Quantum universality by state distillation,” *Quantum Information & Computation* **9** (2009), no. 11 1030–1052.
- [6] J. Haah, M. B. Hastings, D. Poulin, and D. Wecker, “Magic State Distillation with Low Space Overhead and Optimal Asymptotic Input Count,” *arXiv e-prints* (Mar., 2017) [arXiv:1703.07847](#), [1703.07847](#).
- [7] S. Bravyi and J. Haah, “Magic-state distillation with low overhead,” *Phys. Rev. A* **86** (Nov., 2012) 052329, [1209.2426](#).
- [8] E. T. Campbell and M. Howard, “Unifying Gate Synthesis and Magic State Distillation,” *Phys. Rev. Lett.* **118** (Feb., 2017) 060501, [1606.01906](#).
- [9] E. T. Campbell and M. Howard, “Unified framework for magic state distillation and multiqubit gate synthesis with reduced resource cost,” *Phys. Rev. A* **95** (Feb., 2017) 022316, [1606.01904](#).

- [10] E. T. Campbell and M. Howard, “Magic state parity-checker with pre-distilled components,” *arXiv e-prints* (Sept., 2017) arXiv:1709.02214, 1709.02214.
- [11] C. Jones, “Multilevel distillation of magic states for quantum computing,” *Phys. Rev. A* **87** (Apr., 2013) 042305, 1210.3388.
- [12] E. T. Campbell, “Catalysis and activation of magic states in fault-tolerant architectures,” *Phys. Rev. A* **83** (Mar., 2011) 032317, 1010.0104.
- [13] H. Anwar, E. T. Campbell, and D. E. Browne, “Qutrit magic state distillation,” *New Journal of Physics* **14** (2012), no. 6 063006, arXiv:1202.2326.
- [14] E. T. Campbell, H. Anwar, and D. E. Browne, “Magic-State Distillation in All Prime Dimensions Using Quantum Reed-Muller Codes,” *Phys. Rev. X* **2** (Dec, 2012) 041021, arXiv:1205.3104.
- [15] E. T. Campbell, “Enhanced fault-tolerant quantum computing in d-level systems,” *Physical Review Letters* **113** (2014), no. 23 230501, arXiv:1406.3055.
- [16] H. Dawkins and M. Howard, “Qutrit Magic State Distillation Tight in Some Directions,” *Phys. Rev. Lett.* **115** (Jul, 2015) 030501, arXiv:1504.05965.
- [17] S. Prakash, “Magic State Distillation with the Ternary Golay Code,” *arXiv e-prints* (Mar., 2020) arXiv:2003.02717, 2003.02717.
- [18] M. Howard, J. Wallman, V. Veitch, and J. Emerson, “Contextuality supplies the ‘magic’ for quantum computation,” *Nature* **510** (June, 2014) 351–355, arXiv:1401.4174.
- [19] N. Delfosse, C. Okay, J. Bermejo-Vega, D. E. Browne, and R. Raussendorf, “Equivalence between contextuality and negativity of the Wigner function for qudits,” *New Journal of Physics* **19** (dec, 2017) 123024.
- [20] W. van Dam and M. Howard, “Noise thresholds for higher-dimensional systems using the discrete Wigner function,” *Phys. Rev. A* **83** (Mar, 2011) 032310.
- [21] V. Veitch, C. Ferrie, D. Gross, and J. Emerson, “Negative quasi-probability as a resource for quantum computation,” *New Journal of Physics* **14** (nov, 2012) 113011.
- [22] A. Mari and J. Eisert, “Positive Wigner Functions Render Classical Simulation of Quantum Computation Efficient,” *Phys. Rev. Lett.* **109** (Dec, 2012) 230503.
- [23] V. Veitch, S. A. H. Mousavian, D. Gottesman, and J. Emerson, “The resource theory of stabilizer quantum computation,” *New Journal of Physics* **16** (jan, 2014) 013009.
- [24] X. Wang, M. M. Wilde, and Y. Su, “Efficiently computable bounds for magic state distillation,” *arXiv preprint arXiv:1812.10145* (2018).

- [25] A. Mair, A. Vaziri, G. Weihs, and A. Zeilinger, “Entanglement of the orbital angular momentum states of photons,” *Nature* **412** (2001), no. 6844 313.
- [26] R. Bianchetti, S. Filipp, M. Baur, J. M. Fink, C. Lang, L. Steffen, M. Boissonneault, A. Blais, and A. Wallraff, “Control and Tomography of a Three Level Superconducting Artificial Atom,” *Phys. Rev. Lett.* **105** (Nov, 2010) 223601.
- [27] A. B. Klimov, R. Guzmán, J. C. Retamal, and C. Saavedra, “Qutrit quantum computer with trapped ions,” *Phys. Rev. A* **67** (Jun, 2003) 062313.
- [28] G. Kimura, “The Bloch vector for N -level systems,” *Physics Letters A* **314** (Aug, 2003) 339–349, [quant-ph/0301152](#).
- [29] I. P. Mendas, “The classification of three-parameter density matrices for a qutrit,” *Journal of Physics A Mathematical General* **39** (Sep, 2006) 11313–11324.
- [30] I. Bengtsson, S. Weis, and K. Życzkowski, “Geometry of the Set of Mixed Quantum States: An Apophatic Approach,” in *Geometric Methods in Physics* (P. Kielanowski, S. T. Ali, A. Odziejewicz, M. Schlichenmaier, and T. Voronov, eds.), (Basel), pp. 175–197, Springer Basel, 2013. [arXiv:1112.2347](#).
- [31] G. Sarbicki and I. Bengtsson, “Dissecting the qutrit,” *Journal of Physics A Mathematical General* **46** (Jan, 2013) 035306, [1208.2118](#).
- [32] G. N. M. Tabia and D. M. Appleby, “Exploring the geometry of qutrit state space using symmetric informationally complete probabilities,” *Phys. Rev. A* **88** (Jul, 2013) 012131, [1304.8075](#).
- [33] D. P. Srivastava, V. Sahni, and P. S. Satsangi, “From n -qubit multi-particle quantum teleportation modelling to n -qudit contextuality based quantum teleportation and beyond,” *International Journal of General Systems* **46** (2017), no. 4 414–435, <https://doi.org/10.1080/03081079.2017.1308361>.
- [34] S. K. Goyal, B. N. Simon, R. Singh, and S. Simon, “Geometry of the generalized Bloch sphere for qutrits,” *Journal of Physics A: Mathematical and Theoretical* **49** (2016), no. 16 165203.
- [35] M. Howard and J. Vala, “Qudit versions of the qubit $\pi/8$ gate,” *Physical Review A* **86** (2012), no. 2 022316, [arXiv:1206.1598](#).
- [36] M. Howard, “Maximum nonlocality and minimum uncertainty using magic states,” *Phys. Rev. A* **91** (Apr, 2015) 042103.
- [37] X. Wang, M. M. Wilde, and Y. Su, “Quantifying the magic of quantum channels,” *New Journal of Physics* **21** (oct, 2019) 103002.

- [38] D. M. Appleby, “Symmetric informationally complete-positive operator valued measures and the extended Clifford group,” *Journal of Mathematical Physics* **46** (May, 2005) 052107, [quant-ph/0412001](#).
- [39] D. M. Appleby, I. Bengtsson, and S. Chaturvedi, “Spectra of phase point operators in odd prime dimensions and the extended Clifford group,” *Journal of Mathematical Physics* **49** (Jan, 2008) 012102, [0710.3013](#).
- [40] D. M. Appleby, “SIC-POVMS and MUBS: Geometrical Relationships in Prime Dimension,” in *American Institute of Physics Conference Series* (L. Accardi, G. Adenier, C. Fuchs, G. Jaeger, A. Y. Khrennikov, J.-Å. Larsson, and S. Stenholm, eds.), vol. 1101 of *American Institute of Physics Conference Series*, pp. 223–232, Mar, 2009. [0905.1428](#).
- [41] D. M. Appleby, “Properties of the extended Clifford group with applications to SIC-POVMS and MUBs,” *arXiv e-prints* (Sep, 2009) [arXiv:0909.5233](#), [0909.5233](#).
- [42] H. Zhu, “SIC POVMs and Clifford groups in prime dimensions,” *Journal of Physics A: Mathematical and Theoretical* **43** (2010), no. 30 305305.
- [43] M. Planat and Z. Gedik, “Magic informationally complete POVMs with permutations,” *Royal Society open science* **4** (2017), no. 9 170387.
- [44] M. Planat and R. Ul Haq, “The magic of universal quantum computing with permutations,” *Advances in mathematical physics* **2017** (2017).
- [45] M. Planat, R. Aschheim, M. M. Amaral, and K. Irwin, “Universal Quantum Computing and Three-Manifolds,” *Symmetry* **10** (2018), no. 12.
- [46] W. K. Wootters, “A Wigner-function formulation of finite-state quantum mechanics,” *Annals of Physics* **176** (May, 1987) 1–21.
- [47] K. S. Gibbons, M. J. Hoffman, and W. K. Wootters, “Discrete phase space based on finite fields,” *Phys. Rev. A* **70** (Dec, 2004) 062101.
- [48] D. Gross, “Hudson’s theorem for finite-dimensional quantum systems,” *Journal of Mathematical Physics* **47** (Dec., 2006) 122107–122107, [arXiv:quant-ph/0602001](#).
- [49] C. Cormick, E. F. Galvao, D. Gottesman, J. P. Paz, and A. O. Pittenger, “Classicality in discrete Wigner functions,” *Physical Review A* **73** (2006), no. 1 012301.
- [50] S. Prakash and A. Gupta, “Contextual bound states for qudit magic state distillation,” *Phys. Rev. A* **101** (Jan, 2020) 010303.
- [51] E. T. Campbell and D. E. Browne, “On the Structure of Protocols for Magic State Distillation,” in *Theory of Quantum Computation, Communication, and Cryptography* (A. Childs and M. Mosca, eds.), (Berlin, Heidelberg), pp. 20–32, Springer Berlin Heidelberg, 2009.

- [52] E. T. Campbell and D. E. Browne, “Bound States for Magic State Distillation in Fault-Tolerant Quantum Computation,” *Phys. Rev. Lett.* **104** (Jan, 2010) 030503.
- [53] H. Pashayan, J. J. Wallman, and S. D. Bartlett, “Estimating Outcome Probabilities of Quantum Circuits Using Quasiprobabilities,” *Phys. Rev. Lett.* **115** (Aug, 2015) 070501.
- [54] M. Howard, E. Brennan, and J. Vala, “Quantum Contextuality with Stabilizer States,” *Entropy* **15** (Jun, 2013) 23402362.
- [55] V. Sahni, D. Srivastava, and P. Satsangi, “Unified modelling theory for qubit representation using quantum field graph models,” *Journal of the Indian Institute of Science* **89** (07, 2009).
- [56] D. Srivastava, V. Sahni, and P. Satsangi, “Graph-theoretic quantum system modelling for information/computation processing circuits,” *International Journal of General Systems* **40** (11, 2011) 777–804.
- [57] M. Howard and E. Campbell, “Application of a Resource Theory for Magic States to Fault-Tolerant Quantum Computing,” *Phys. Rev. Lett.* **118** (Mar., 2017) 090501, 1609.07488.
- [58] M. Beverland, E. Campbell, M. Howard, and V. Kliuchnikov, “Lower bounds on the non-Clifford resources for quantum computations,” *arXiv e-prints* (Apr., 2019) arXiv:1904.01124, 1904.01124.
- [59] J. E. Humphreys, “Representations of $SL(2,p)$,” *Amer. Math. Monthly* **82** (1975) 21–39.
- [60] A. Acín, T. Fritz, A. Leverrier, and A. B. Sainz, “A Combinatorial Approach to Nonlocality and Contextuality,” *Communications in Mathematical Physics* **334** (Mar, 2015) 533–628.
- [61] S. Prakash, A. Jain, B. Kapur, and S. Seth, “Normal form for single-qutrit Clifford+ T operators and synthesis of single-qutrit gates,” *Phys. Rev. A* **98** (Sep, 2018) 032304.